Am J Cancer Res 2019;9(12):2580-2598
www.ajcr.us /ISSN:2156-6976/ajcr0104433

Original Article

Glucocorticoid receptor antagonism overcomes resistance to BRAF inhibition in BRAF^{V600E}-mutated metastatic melanoma

José M Estrela[1], Rosario Salvador[1], Patricia Marchio[1], Soraya L Valles[1], Rafael López-Blanch[1], Pilar Rivera[1], María Benlloch[2], Javier Alcácer[3], Carlos L Pérez[4], José A Pellicer[1], Elena Obrador[1]

[1]Department of Physiology, University of Valencia, Valencia 46010, Spain; [2]Department of Health & Functional Valorization, San Vicente Martir Catholic University, Valencia 46001, Spain; [3]Pathology Laboratory, Quirón Hospital, Valencia 46010, Spain; [4]Department of Biochemistry, Institute of Basic and Preclinical Sciences Victoria de Girón, La Habana 3102146, Cuba

Received November 4, 2019; Accepted November 18, 2019; Epub December 1, 2019; Published December 15, 2019

Abstract: Clinical applications of glucocorticoids (GC) in Oncology are dependent on their pro-apoptotic action to treat lymphoproliferative cancers, and to alleviate side effects induced by chemotherapy and/or radiotherapy. However, the mechanism(s) by which GC may also promote tumor progression remains unclear. GC receptor (GR) knockdown decreases the antioxidant protection of highly metastatic B16-F10 melanoma cells. We hypothesize that a GR antagonist (RU486, mifepristone) could increase the efficacy of BRAF-related therapy in BRAF^{V600E}-mutated metastatic melanoma. *In vivo* formed spontaneous skin tumors were reinoculated into nude mice to expand the metastases of different human BRAF^{V600E} melanoma cells. The GR content of melanoma cell lines was measured by [^{3}H]-labeled ligand binding assay. Nuclear Nrf2 and its transcription activity was investigated by RT-PCR, western blotting, and by measuring Nrf2- and redox state-related enzyme activities and metabolites. GR knockdown was achieved using lentivirus, and GR overexpression by transfection with the NR3C1 plasmid. shRNA-induced selective Bcl-xL, Mcl-1, AKT1 or NF-κB/p65 depletion was used to test the efficacy of vemurafenib (VMF) and RU486 against BRAF^{V600E}-mutated metastatic melanoma. During early progression of skin melanoma metastases, RU486 and VMF induced a drastic metastases regression. However, treatment at an advanced stage of growth demonstrated the development of resistance to RU486 and VMF. This resistance was mechanistically linked to overexpression of specific proteins of the Bcl-2 family (Bcl-xL and Mcl-1 in our experimental models). We found that melanoma resistance is decreased if AKT and NF-κB signaling pathways are blocked. Our results highlight mechanisms by which metastatic melanoma cells adapt to survive.

Keywords: Melanoma, oxidative stress, BRAF, glucocorticoids, Nrf2, Bcl-2

Introduction

Metastatic melanoma is the least common skin cancer, but the most deadly because it spreads quickly and easily to other parts of the body [1]. Despite the availability of new targeted therapies, a significant unmet need in the treatment of advanced melanoma remains [2].

GC are widely used in cancer therapy due to their pro-apoptotic properties in different tumor cells [3]. However GC may also induce a yet undefined resistant phenotype, thereby facilitating fast growth and metastases of different solid tumors [3, 4]. It has been observed that GC, at pathophysiological concentrations (non-therapeutic), can induce anti-apoptotic signals that are associated with resistance to apoptosis of cells of epithelial origin and of most of malignant solid tumors submitted to cytotoxic therapy [5-7]. This apparent biological paradox could hypothetically reflect a difference in circulating GC levels. Where pathophysiological levels (e.g. those measured in the presence of a growing tumor) are lower than those reached if GC are administered (IV or IM) at pharmacological doses.

We reported that GR knockdown diminishes the antioxidant protection of highly metastatic

B16-F10 melanoma cells and, thereby, causes a drastic decrease in their survival during interaction with vascular endothelial cells (which release reactive oxygen and nitrogen species) [8]. *In vivo* only 10% of the B16-F10 cells attached to the endothelium survived within the hepatic microcirculation (compared to 90% survival in the controls) [8].

The $BRAF^{V600E}$ mutation is the most commonly observed in patients, confers constitutive kinase activity, accounts for > 90% of BRAF mutations in melanoma, and is detected very early in melanoma development [9]. Interestingly, recent studies reveal that VMF/PLX4032 (a selective inhibitor of mutant $BRAF^{V600E}$) increases mitochondrial respiration and reactive oxygen species (ROS) production in $BRAF^{V600E}$ melanoma cell lines [10]. Thus we tested the hypothesis that combination of a GR antagonist and VMF could induce regression of melanoma metastases.

Materials and methods

Culture of melanoma cells

Human A2058, COLO-679 and SK-Mel-28 melanoma cells were from the ATCC (Manassas, VA). Cells were grown in DMEM (Invitrogen, San Diego, CA), pH 7.4, supplemented with 10% heat-inactivated FCS (Biochrom KG, Berlin, Germany), 100 units/mL penicillin and 100 µg/mL streptomycin. Cells were plated (20,000 cells/cm^2) and cultured at 37°C in a humidified atmosphere with 5% CO_2. Cells were harvested by incubation for 5 min with 0.05% (w/v) trypsin (Sigma Aldrich, St. Louis, MO) in PBS, pH 7.4, containing 0.3 mM EDTA, followed by the addition of 10% FCS to inactivate the trypsin. Cells were allowed to attach for 12 h before any treatment addition. Cell number and viability were determined using a BioRad (Hercules, CA) TC20 Automated Cell Counter.

Animals and experimental metastases

Nude (nu/nu) mice (male, 9-10 weeks old, Charles River Laboratories, Wilmington, MA) were fed *ad libitum* on a standard diet (Letica, Rochester Hills, MI), and kept on a 12-h-light/12-h-dark cycle with the room temperature at 22°C. Procedures were in compliance with international laws and policies (EEC Directive 86/609, OJ L 358. 1, December 12, 1987; and NIH Guide for the Care and Use of Laboratory Animals, NIH Publ. No. 85-23, 1985).

Skin metastases were reproduced by orthotopic intradermic inoculation of metastatic A2058 or COLO-679 melanoma cells. Metastatic melanoma cells were isolated (see below) from spontaneous skin metastases found in nu/nu mice s.c. xenografted with these tumors. The initial s.c. xenografted tumors were allowed to grow for 3 weeks and then were surgically removed. Spontaneous skin metastases were detected (in 10-15% of all mice and in different areas of skin to the initial location of the xenografts) 2-3 months later.

To generate orthotopic xenografts mice were inoculated intradermically (on the back) with 2×10^6 metastatic melanoma cells per mouse. During the time frame of our experiments, the reinoculated metastatic cells grew as a single tumor. Tumor volume was measured using calipers, and expressed in mm^3 according to $V = 0.5a \times b^2$ (a and b are the long and short diameters, respectively). For histological analysis skin tumors were fixed in 4% formaldehyde in PBS (pH, 7.4) for 24 h at 4°C, paraffin embedded, and stained with hematoxilin & eosin and safran. The sacrifice was performed by cervical dislocation.

RU486 and vemurafenib administration to tumor-bearing mice

Based on published human and murine pharmacokinetics, dosage used to treat Cushing's syndrome in humans (300-1200 mg of RU486, oral, once a day), and FDA's recommendations for murine equivalent doses (www.fda.gov), we calculated a clinically relevant dose of 10 mg RU486/kg of mouse which was administered i.p., once a day, in 7-8 µL of dimethyl formamide per mouse.

The recommended dose of VMF in cancer patients is 960 mg (oral, twice a day) [11], and following the same criteria used for RU486, we calculated a clinically relevant dose of 45 mg VMF/kg of mouse. VMF, formulated in the same high-bioavailability microprecipitated bulk powder formulation used in patients, was suspended in an aqueous vehicle containing 2% Klucel LF (Hercules Inc., Wilmington, DE) and adjusted to pH 4 with dilute HCl. Vehicle control and VMF were given orally (once a day) using a sterile

1-mL syringe and 18-gauge gavage needle (200 µL per mouse) at the dose indicated above.

Isolation of tumor cells from skin metastases using enzymatic digestion and a double Ficoll gradient

To maximize cell yield and viability we used collagenase III (200 U/mL; Sigma-Aldrich), DNase I (200 U/mL; Sigma-Aldrich) and trypsin (5 mg/mL; Invitrogen), and a non-enzymatic dissociation buffer (NEDB, Invitrogen). The mice were killed, and the tumors were removed into cold culture media. The tumors were minced into 1-3 mm fragments, and then incubated with the dissociation solution (see above) × 30 min at 37°C. The tumor fragments were mixed up and down every 10 min using a 1000 µL micropipette with a tip. After each incubation, the fragments were filtered through a 40 mm nylon mesh cell strainer (BD Biosciences, San Diego, CA). The released cells were centrifuged at 1200 rpm × 2 min and stored in cold CO_2-independent medium with 30% FCS at 4°C. Fresh dissociation solution was added to the remaining tissue fragments for 30 min. The fragments were pushed through a sieve. The dissociated cells were layered onto a double Ficoll gradient (Histopaque; Sigma Aldrich; densities 1.077 and 1.119) and spun at 700 × g for 30 min at room temperature. Cells removed from both interfaces were pooled and washed two times in CO_2-independent medium and stored at 4°C.

Measurement of the GR content of melanoma cell lines by [^{3}H]-labeled ligand binding assay

The GR content was measured by a whole-cell binding assay as previously described [12]. The melanoma cells were exposed to various concentrations of [^{3}H]-dexamethasone (DXM) (GE Healthcare Life Sciences, Björkgatan, Uppsala, Sweden) in the presence or absence of unlabeled DXM. Using the specific activity of [^{3}H]-DXM, the GR number/cell was calculated, assuming that each receptor binds to one DXM molecule.

Enzyme assays

Isolated tumor cells were homogenized in 0.1 M phosphate buffer (pH 7.2) at 4°C. γ-glutamylcysteine ligase (GCL), GSH synthase (GSS), glutathione peroxidase (GPX), glutathione S transferase (GST), thioredoxin reductase (TXNRD), superoxide dismutase 1 and 2 (SOD1 and SOD2), catalase (CAT), and NADPH oxidase 1 (NOX 1) activities were measured following previously reported methodology [12]. Protein concentration was determined with the Pierce BCA protein assay (Thermo Fisher Scientific, Waltham, MA).

Measurement of H_2O_2 and $O_2^{\cdot-}$

Quantitative measurement of H_2O_2 and flow cytometric determination of $O_2^{\cdot-}$-generation were performed as previously described [12].

Glutathione, glutathione disulfide, thioredoxin, $NADP^+$, and NADPH determination

GSH (glutathione, γ-L-glutamyl-L-cystenyl-glycine) and GSSG (glutathione disulfide) were determined by LC/MS as previously reported [8]. Thioredoxin (TXN) was quantitated using an assay kit from Cayman Chemical (Ann Arbor, MI). $NADP^+$ and NADPH were quantitated using an assay kit from Sigma Aldrich.

Lipid peroxidation

For isoprostane determination, tumor samples were homogenized in 0.1 M phosphate buffer (pH 7.4)+1 mM EDTA+0.005% butylated hydroxytoluene. Isoprostanes were measured using the 8-isoprostane EIA kit (Cayman Chemical) and following the manufacturer's protocol.

RT-PCR and detection of mRNA

Total RNA was isolated using the TRIzol kit from Invitrogen following the manufacturer's instructions. cDNA was obtained using a random hexamer primer and a MultiScribe Reverse Transcriptase kit as recommended by the manufacturer (Taq-Man RT Reagents; Applied Biosystems, Foster City, CA). PCR master mix and AmpliTaq Gold DNA polymerase (Applied Biosystems) were added to the primers previously reported [12]. Real-time quantification of mRNA relative to glyceraldehyde 3-phosphate dehydrogenase (GAPDH) was performed as previously reported [12].

Western blots

Western blot analysis was performed as previously described [12]. Proteins were transferred

to a nitrocellulose membrane and subjected to western blotting with specific anti-human monoclonal antibodies (OriGene, Rockville, MD; and Santa Cruz Biotechnology, Dallas, TX). Blots were developed using horseradish peroxidase-conjugated secondary antibody and enhanced chemiluminescence (ECL system; GE Health Care Life Sciences). Protein bands were quantified using laser densitometry.

Nrf2 gene transfer and measurement

The Tet-Off Advanced Inducible Gene Expression System (Clontech, Mountain View, CA) was used, as previously described [12], to insert the human Nrf2 [nuclear factor (erythroid-derived 2)-like 2] gene and for transfection into melanoma cells. The NE-PER extraction kit from Thermo Fisher Scientific was used for nuclear protein extraction according to the manufacturer's instructions.

Immunohistochemistry and cell death analysis

Mouse anti-human HMB45 monoclonal antibodies (Abcam, Cambridge, UK) were used for immunohistochemical detection of human melanoma cells; whereas monoclonal mouse anti-human Ki-67 antibodies (Dako, SantCugat del Vallés, Spain) were used for immunohistochemical detection of the tumor-growing fraction (see [12]). DNA strand breaks in apoptotic cells were assayed using a TUNEL labeling assay (Roche, Basel, Switzerland), fluorescence microscopy and manufacturer's methodology. Apoptotic and necrotic cell death were distinguished by using fluorescence microscopy as previously described [13].

Glucocorticoid receptor knockdown: lentivirus production, titering, and transduction of target cell lines

HEK-293T cells (ATCC) used for lentiviral production were grown in DMEM containing 10% FBS, 4.5 g/l glucose, 50 U/ml penicillin, 50 mg/ml streptomycin, 1 mM sodium pyruvate, 4 mM L-glutamine, and 0.1 mM non-essential amino acids. The procedure followed methodology previously reported in detail [8]. Cells transfected with retroviral vector harboring the GFP gene were used as a negative control. Established clones were grown as described above in medium supplemented with 0.5 mg/ml puromycin. Silencing was confirmed by immunoblotting. The anti-human GR monoclonal antibodies were purchased from Santa Cruz Biotechnology.

GR overexpression and analysis

GR overexpression was induced by transfecting the melanoma cells with nuclear receptor subfamily 3 group C member 1 [Homo sapiens nuclear receptor subfamily 3 group C member 1 (NR3C1), transcript variant 1, mRNA]-encoding DNA plasmids as previously described for human triple-negative breast cancer cells [14]. The coding sequence (CCDS4278.1) of the predominant glucocorticoid receptor gene NR3C1 transcript variant 1 (NM_000176.2) was synthesized with the restriction sites KpnI and XhoI on the 5' and 3' end, respectively (InvivoGen, San Diego, CA), and cloned in frame into the pcDNA6/V5-His A vector (Life Technologies, Alcobendas, Spain). The cells were transfected with the NR3C1 plasmid (0.4 μg) for 24 h using Lipofectamine 2000 transfection reagent (Invitrogen). Following 30 h of cultivation, the cells had reached 90% confluency, and were rinsed once with HBSS before proceeding to total RNA extraction. The GR content was measured by a whole-cell binding assay as described above.

Measurement of corticosterone and dexamethasone

Plasma levels of corticosterone (Kamiyama Biomedical Co., Seattle, WA) and DXM (Bioo Scientific, Austin, TX) were quantified by ELISA according to the suppliers' instructions.

Evaluation of drug-induced in vivo toxicity

This included the following parameters: blood cell count and chemistry based on NIH standard methodology, and urinalysis based on the Combur test from Roche. Urine pH was directly measured using a pH meter and urine protein content with the Pierce BCA Protein Assay Kit. The glomerular filtration rate (GFR) was evaluated following the single bolus FITC-inulin clearance methodology described for mice by [15].

Isolation and incubation of hepatocytes and lymphocytes

Isolation procedures followed previously reported methodology [16, 17]. Rates of glucose and

glutamine utilization were measured as previously described [18].

Culture of hepatocytes

Isolated hepatocytes were diluted with warm William's complete medium to 2.5 × 10^5 cells/mL, and plated in un-coated cultured flasks at a ratio of 5 × 10^5 cells/cm^2. Cells were cultured at 37°C in a humidified atmosphere of 95% air and 5% CO_2.

shRNA expression vectors

HEK-293T cells (ATCC) used for lentiviral production were grown in DMEM containing 10% FBS, 4.5 g/L glucose, 50 U/mL penicillin, 50 mg/mL streptomycin, 1 mM sodium pyruvate, 4 mM L-glutamine, and 0.1 mM non-essential amino acids. The LENTI-Smart system from InvivoGen was used according to the manufacturer's protocol [bcl-xL shRNA, mcl-1 shRNA, AKT1 shRNA, and NF-κB/p65 shRNA were designed from the Ensemble genome browser/database (Ensembl, the Wellcome Trust Genome Campus, Cambridge, UK) to target the following blc-xl, mcl-1 gene, AKT1, NF-κB/p65 sequences: bcl-xl, 5'-GGAGATGCAGGTATTGGTGAG-3'; mcl-1, 5'-ACGCGGTAATCGGACTCAA-3'; AKT1, 5'-TGACCATGAACGAGTTTGA-3', NF-κB/p65, 5'-GGATCCTGTGTCCATTGTCTCACTCCTCGAGGAGTGAGACAATGGACACATTTTTTTGAATTC-3']. Scrambled sequences were used as controls. Cells transfected with lentiviral vectors not harboring any gene (InvivoGen) were used as negative controls. Lentiviral particles were collected 48 h after transfection. Cell/viral debris was removed from the collected supernatants by centrifugation (2000 rpm × 65 min) and filtration using a 0.45 mm PVDF (low protein binding) filter. Lentiviral particles were concentrated by ultracentrifugation (70000 × g for 2 h at 4°C). The fibrosarcoma cell line HT1080 (ATCC) was used for titering lentiviral vectors using the GFP within the transfer construct as a marker for microscopic analysis. Lentiviral vectors contain the viral capsid protein (p24), which is encoded by the gag gene. An ELISA was used to determine the amount of p24 in the supernatant. Forty-eight hours following viral transduction, the number of GFP-positive colonies per well was counted by fluorescence microscopy. Transducing units per milliliter was calculated as follows: (T × V)/N, where T is the titer of the lentiviral vector stock, V is the volume of lentiviral vectors (in mL), and N is the number of cells to be transduced. Melanoma cell variants were transduced and subsequently selected by puromycin treatment to produce melanoma bcl-xl, mcl-1, AKT1, or NF-κB/p65 shRNA cell variants. Clonal populations of each cell line were obtained by flow cytometric cell sorting. Cells transfected with retroviral vector harboring the GFP gene were used as a negative control. Established clones were grown as described above in medium supplemented with 0.5 mg/mL puromycin. Silencing was confirmed by immunoblotting. The anti-human Bcl-xl, Mcl-1, AKT1, and NF-κB/p65 monoclonal antibodies were from Santa Cruz Biotechnology.

Nuclear factor-κB DNA binding

Nuclear factor-κB (NF-κB) p50/65 DNA binding activity in nuclear extracts was carried out to measure the degree of NF-κB activation. Nuclear extract was prepared using the NE-PER™ Nuclear and Cytoplasmic Extraction procedure of Thermo Fisher Scientific, and following manufacturer's instructions. An ELISA was done in line with the manufacturer's protocol for a commercial kit (Chemiluminescent NF-κB p50/65 Transcription Factor Assay, Oxford Biomedical Research, Rochester Hills, MI). Antibodies anti-cyclin D1 were used as negative controls.

Statistics

Data are presented as mean values ± SD for the number of different experiments. Statistical analyses were performed using Student's t-test, and $P < 0.05$ was considered significant.

Results

Effect of RU486 on the antioxidant defense system of in vivo growing $BRAF^{V600E}$-mutated metastatic melanoma cells

Human melanoma cells express high-affinity GR [19]. We investigated if pharmacologically relevant doses of RU486 (mifepristone, a GR antagonist) [20] could decrease the antioxidant protection of human $BRAF^{V600E}$ melanoma cell lines.

After the initial xenografted tumors were removed, *in vivo* formed spontaneous skin tumors

Table 1. Effect of RU486 on different Nrf-2- and redox state-related enzyme activities and metabolites in metastatic $BRAF^{V600E}$-mutated melanoma cells growing *in vivo*

	iA2058		iCOLO-679	
	-	RU486	-	RU486
GSH and TXN				
GCL (mU/10⁶ cells)	146 ± 31	79 ± 26#	192 ± 49	102 ± 36*
GSS (mU/10⁶ cells)	19.2 ± 4.5	11.4 ± 2.9*	25.6 ± 6.6	14.7 ± 3.4#
GPX (mU/10⁶ cells)	6.5 ± 1.2	3.7 ± 1.1#	5.4 ± 1.0	2.1 ± 0.5#
GSR (mU/10⁶ cells)	11.7 ± 2.4	8.7 ± 1.5	13.8 ± 1.9	8.0 ± 2.3*
GST (mU/10⁶ cells)	12.3 ± 2.0	5.0 ± 1.3#	10.4 ± 1.9	4.3 ± 1.4#
GGT (mU/10⁶ cells)	26.1 ± 5.0	24.7 ± 5.5	33.9 ± 7.4	30.6 ± 6.0
GSH (nmol/10⁶ cells)	27.5 ± 4.1	13.4 ± 2.7#	44.8 ± 8.3	19.5 ± 3.7#
GSSG (nmol/10⁶ cells)	0.2 ± 0.1	0.3 ± 0.1	0.2 ± 0.05	0.3 ± 0.1
TXN (μg/10⁶ cells)	1.5 ± 0.4	0.9 ± 0.3*	1.9 ± 0.5	0.9 ± 0.2#
TXNRD (U/10⁶ cells)	1.7 ± 0.3	1.0 ± 0.2*	2.1 ± 0.6	0.9 ± 0.2#
ROS				
SOD1 (U/10⁶ cells)	1.7 ± 0.3	0.8 ± 0.2#	1.9 ± 0.4	0.8 ± 0.15#
SOD2 (U/10⁶ cells)	0.2 ± 0.1	0.15 ± 0.05	0.3 ± 0.1	0.2 ± 0.1
CAT (mU/10⁶ cells)	3.1 ± 0.7	1.2 ± 0.2#	3.8 ± 0.5	1.3 ± 0.4#
NOX (R.L.U./10⁶ cells)	147 ± 36	157 ± 44	155 ± 26	133 ± 31
H_2O_2 (nmol/10⁶ cells x min)	1.4 ± 0.3	1.2 ± 0.2	2.0 ± 0.3	1.8 ± 0.2
$O_2^{\cdot-}$ (ΔFL1, a.u.)	1.9 ± 0.5	4.5 ± 0.9#	2.4 ± 0.5	5.9 ± 1.2#
NADPH supplying dehydrogenases				
G6PDH (mU/10⁶ cells)	725 ± 102	466 ± 69#	857 ± 136	490 ± 77#
ME (mU/10⁶ cells)	89 ± 15	47 ± 10#	72 ± 17	38 ± 11#
IDH (U/10⁶ cells)	2.0 ± 0.3	1.2 ± 0.3*	1.7 ± 0.5	1.4 ± 0.2
Redox state				
NADPH (nmol/mg prot.)	0.16 ± 0.04	0.1 ± 0.005#	0.2 ± 0.06	0.12 ± 0.02*
$NADP^+$ (nmol/mg prot.)	0.01 ± 0.005	0.01 ± 0.005	0.01 ± 0.005	0.01 ± 0.002
GSH/GSSG	138 ± 15	45 ± 11#	224 ± 36	66 ± 18#
NADPH/$NADP^+$	16.2 ± 2.5	10.1 ± 1.6#	20.3 ± 3.7	12.3 ± 4.5*

Tumor-bearing mice were treated with vehicle (controls) or RU486 (10 mg/kg IP, QD, see under Materials and Methods). RU486 was administered for 3 weeks starting one week after intradermic inoculation of the cancer cells. All parameters were measured in melanoma cells isolated from tumors 28 days after inoculation. Data are mean values SD for six to seven different tumors per parameter and experimental condition. *$P < 0.05$, #$P < 0.01$, comparing cells isolated from RU486-treated mice vs. controls. CAT, catalase; GCL, γ-glutamylcysteine ligase; GGT, γ-glutamyltranspeptidase; GSR, glutathione reductase; GSS, GSH synthase; NOX, NADPH oxidase; GPX, glutathione peroxidase; Nrf2, nuclear factor (erythroid-derived 2)-like 2; ROS, reactive oxygen species; SOD, superoxide dismutase.

were intradermically reinoculated into mice to expand the experimental metastases (see under Experimental procedures). Three different human $BRAF^{V600E}$ melanoma cells were used (A2058, COLO-679 and SK-Mel-28, see Table S1 (available on request from the corresponding author) for their genetic background). However only A2058 and COLO-679 cells generated spontaneous metastases.

As shown in **Table 1**, administration of RU486 (10 mg/kg IP, QD) to mice bearing metastatic $BRAF^{V600E}$-mutated (iA2058 and iCOLO-679) melanoma cells caused in both tumors a decrease in different Nrf2- and redox state-related enzyme activities and metabolites, i.e. GCL, GSS, GPX, GST, GSH, TXN, TXNRD, SOD1, CAT, and different NADPH supplying dehydrogenases; and a parallel increase in the generation of superoxide anion radicals ($O_2^{\cdot-}$). As compared to the controls (untreated metastatic tumor-bearing mice) expression of practically all tested Nrf2-dependent enzymes, excepting NOX1, decreased in RU486-treated mice bear-

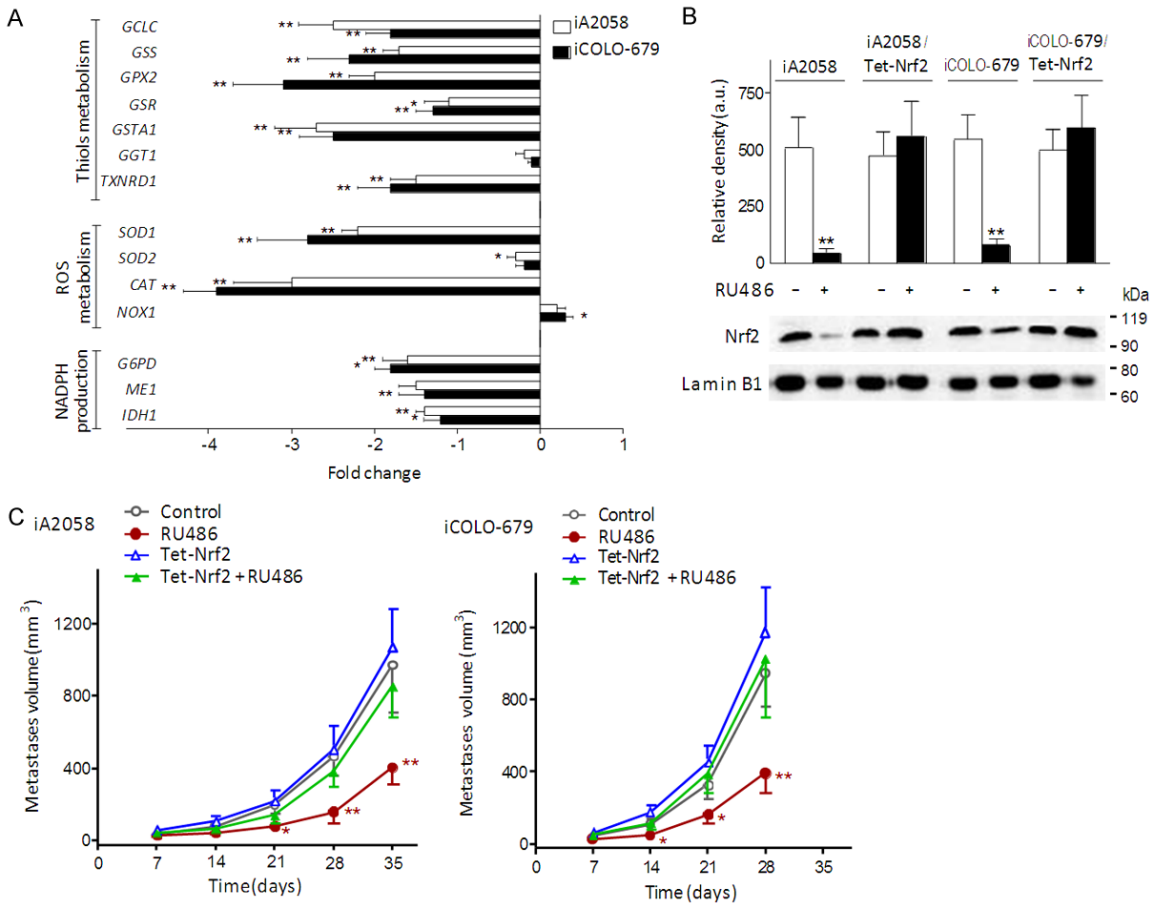

Figure 1. Effect of RU486 on nuclear Nrf2 and its transcription activity in metastatic BRAF^{V600E}-mutated melanoma-bearing mice. (A) Expression of different Nrf2-dependent genes in isolated iA2058 and iCOLO-679 cells from RU486-treated tumor-bearing mice (as in **Table 1**) was compared vs. control tumor-bearing mice treated with physiological saline (*P < 0.05, **P < 0.01). All data, expressing fold change (quantitative RT-PCR), show mean values ± SD for five to six different experiments. (B) Effect of RU486 treatment on the nuclear accumulation of Nrf2 (western blots) in *in vivo* growing iA2058, iA2058/Tet-Nrf2, iCOLO-679, and iCOLO-679/Tet-Nrf2 cells (mean values ± SD for five different experiments (**P < 0.01, comparing RU486 treatment vs. controls). An empty vector (the regulatory plasmid pTett-Off without the Nrf2 gene sequence) was used as a control. Results obtained in cells transfected with this empty vector were not significantly different from those obtained in the control iA2058 and iCOLO-679 cells. (C) Effect of Nrf2 overexpression (see under Materials and Methods) on the tumor growth of control and RU486-treated iA2058- and iCOLO-679-bearing mice. Results obtained in these cells transfected with lentiviral vector not harboring any gene (negative control) were not different from control values. Data are mean values ± SD from five to six different experiments (*P < 0.05, **P < 0.01, comparing RU486 treatment vs. controls. For experiments (B) and (C) no significant differences were found when iA2058/Tet-Nrf2 cells or iCOLO679/Tet-Nrf2 ± RU486 treatment, were compared with control untreated cells.

ing iA2058 or iCOLO-679 melanoma cells (**Figure 1A**). RU486 treatment also associated with an increase of isoprostanes (a marker of oxidative stress) in the cancer cells (Figure S1, available on request from the corresponding author).

As shown in **Figure 1B**, and compared to control melanoma-bearing mice, these effects associated with a decrease in nuclear Nfr2 in metastatic melanoma cells from *in vivo* RU486-treated mice. Moreover, melanoma cells engineered to overexpress Nrf2 were able to grow *in vivo* as controls, despite treatment with RU486 (**Figure 1C**). As shown in Figure S2 (available on request from the corresponding author), in melanoma cells engineered to overexpress Nrf2, expression of all Nrf2-dependent practically returned to control values (close to those found in control tumor-bearing mice treated with physiological saline) despite treatment with RU486 (see also **Figure 1**). RU486

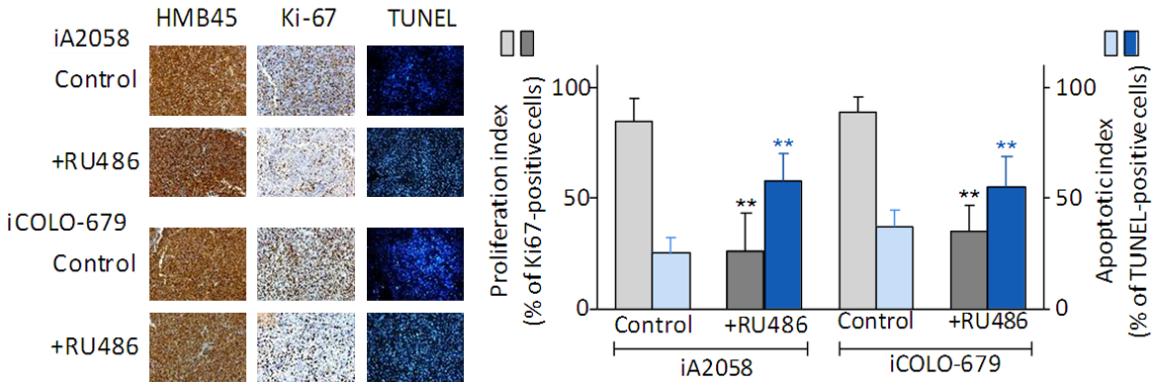

Figure 2. Effect of RU486 on the rates of tumor cell proliferation and apoptotic death *in vivo*. For each experimental condition, a representative picture is shown: immunohistochemical detection of melanoma cells using HMB45 monoclonal antibodies, cell proliferation detection using anti-Ki-67 monoclonal antibodies, and TUNEL staining showing melanoma cells with apoptotic nuclei. Proliferation and apoptotic indexes (expressed as % of Ki-67- and TUNEL-positive cells relative to controls, respectively) were calculated using ten 10 × 10-mm^2 sections per tumor and randomly selecting four different areas per section. All data are mean values ± SD of seven to eight different animals or experiments (**P < 0.01, comparing RU486-treated mice vs. controls).

administration caused a decrease in melanoma cell proliferation (Ki-67 staining) and an increase in apoptotic cell death (TUNEL) (**Figure 2**). The number of GR in iA2058 and iCOLO-679 melanoma cells was of 87 ± 11 and 69 ± 7 × 10^3 GR/cell (n = 6-7 different determinations in each case), respectively. These numbers of GR were similar in control A2058 and COLO-679 cells (83 ± 9 × 10^3 and 63 ± 8 × 10^3 GR/cell, respectively, n = 6-7), and were not significantly affected by the *in vivo* treatment with RU486 (90 ± 10 × 10^3 GR/iA2058 cell and 72 ± 11 × 10^3 GR/COLO-679 cell, n = 7) or by Nrf2 gene transfer-induced Nrf2 overexpression (80 ± 11 × 10^3 GR/iA2058 cell and 61 ± 7 × 10^3 GR/COLO-679 cell, n = 6).

These results, indicating a clear link between Nrf2-dependent transcription activity and the GR antagonist-induced inhibition of metastatic melanoma growth, may be particularly relevant since Nrf2 can increase in e.g. lung carcinoma [21] or melanoma [22] cell proliferation and pharmacological resistance.

Combined GR antagonism and BRAF inhibition promotes regression of early melanoma metastases

Common oncogenes, such as KRAS, BRAF and MYC, increase the transcription and activity of Nrf2 causing an increase in tumor cell protection and, most notably, a decrease in ROS levels [23]. The finding that BRAF stimulates transcription of Nrf2 by elevating levels of JUN, which in turn binds to known start sites for transcription of Nrf2, indicates that some of these effects are direct [23]. These evidences (in addition to its known role in regulating the MAP kinase/ERKs signaling pathway) prompted us to investigate if BRAF inhibition could potentiate the antitumor effect elicited by the GR antagonist. As shown in **Figure 3**, combined treatment with RU486 and vemurafenib (VMF; which specifically interrupts the BRAF/MEK step in the BRAF/MEK/ERK pathway if the BRAF has the common V600E mutation) induced a complete inhibition of BRAF^{V600E}-mutated metastatic melanoma growth under *in vivo* conditions. VMF-induced BRAF downregulation was confirmed by western blot (see **Figure 4**). However early or late administration of VMF alone (7 or 14 days, respectively, after inoculation) did not decreased significantly the rate of metastatic melanoma growth as compared to controls (**Figure 3** displays the results obtained after early administration). Tumor growth inhibition was observed if RU486 and VMF were administered simultaneously and starting 7 days after melanoma inoculation (**Figure 3**). If administration of VMF was delayed and started 14 days after melanoma inoculation the inhibitory effect of the association practically disappeared (**Figure 3**). This difference depending on whether VMF administration is performed early or late suggests that during its *in vivo* growth, and despite the treatment with RU486, metastatic melanoma spon-

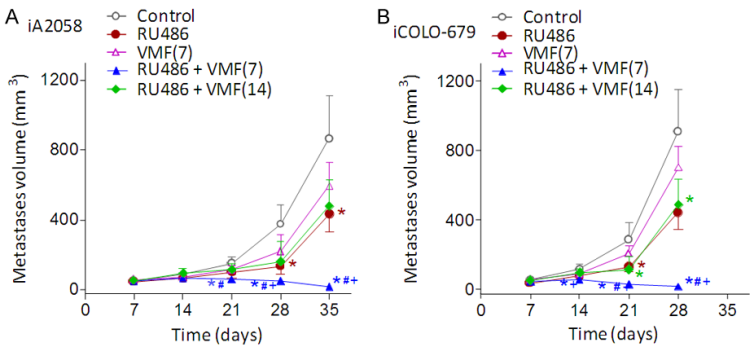

Figure 3. Effect of RU486 and/or vemurafenib treatment on metastatic $BRAF^{V600E}$-mutated melanoma growth. RU486 was administered for 3 weeks (from day 7 to day 28, as in **Table 1**). VMF (45 mg/kg QD, see under Materials and Methods) was administered for 3 weeks starting on day 7 after intradermic inoculation [VMF (7)] of the cancer cells; or 2 weeks starting on day 14 after inoculation [VMF (14)]. All data are mean values ± SD of 9-10 different animals in all groups (*$P < 0.05$, comparing RU486- and/or VMF-treated mice vs. controls; #$P < 0.05$ comparing RU486+VMF-treated vs. RU486-treated; +$P < 0.05$ comparing RU486+VMF-treated vs. VMF-treated).

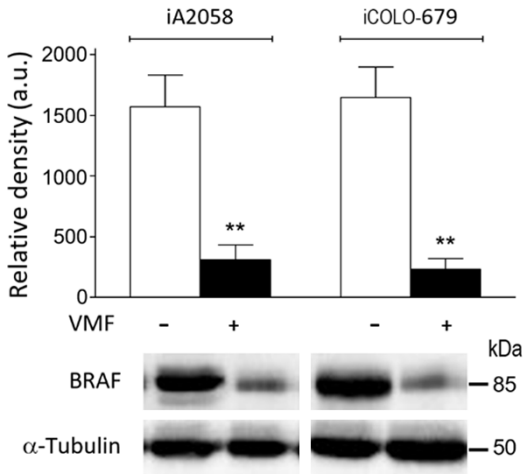

Figure 4. Vemurafenib decreases BRAF levels in metastatic $BRAF^{V600E}$-mutated melanoma tumors. VMF (45 mg/kg QD, see under Experimental procedures) was administered for 2 weeks starting on day 7 after intradermic inoculation. Protein levels (western blots) were measured in metastatic cells 21 days after inoculation (n = 4-5, **$P < 0.01$, comparing cells isolated from VMF-treated mice vs. controls).

taneously develops anti-VMF resistance mechanisms. In our models, resistance to VMF was associated with late administration of VMF. Based on our results, possible differences in BRAF signaling do not seem to explain why if administration of VMF was started 14 days after melanoma inoculation the inhibitory effect of the association (RU486+VMF) practically disappeared.

It is a known fact that the antitumorigenic effects elicited by VMF are short-lived and that the majority of patients present tumor relapse in a short period after treatment [24].

The effects of RU486 are GR dependent

RU-486 (used for medical abortion) is a steroidal antiprogestogen, as well as an antiglucocorticoid, and antiandrogen to a much lesser extent ([20] and refs. therein). It is obviously critical to elucidate if the anti-metastatic effects of RU-486 are totally or partially dependent on GR. As shown in **Figure 5A** and **5B** GR knockdown (see also **Figure 5C** and **5D**) or treatment with RU486 rendered similar results in both melanoma cell lines. However, metastatic growth was not significantly different in control or melanoma cells overexpressing the GR (**Figure 5A-C**). A fact probably indicating that the number of GR present in control cells already ensure a full GR-dependent effect.

We investigated if administration of a specific GR agonist (such as DXM) protects melanoma from cells from VMF. As shown in **Figure 6** plasma levels of corticosterone (the main circulating glucocorticoid in mice [25]) and DXM, as well as metastatic tumor growth, were measured after the administration of DXM (the dose was selected taking into account that plasma levels should reflect pathophysiological conditions in mice). DXM administration decreased corticosterone levels in the plasma of melanoma-bearing mice (**Figure 6C**). As shown in **Figure 6A** and **6B**, the effect of VMF on metastatic tumor growth was abolished by DXM.

Anti-death adaptations related to the Bcl-2 family of proteins in advanced $BRAF^{V600E}$-mutated melanoma metastases

Most mechanisms of acquired melanoma resistance involve reactivation of the MAPK pathway due to events that can occur upstream, downstream, or at the level of BRAF; the PI3K-PTEN-AKT pathway constitutes a second core resistance pathway, which often overlaps with the MAPK pathway [26]. Interestingly, in progress-

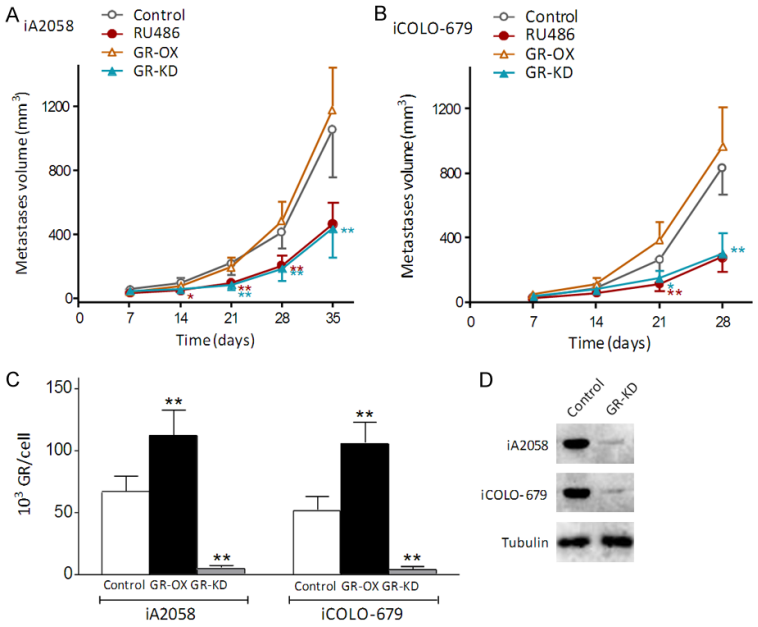

Figure 5. Effect of GR overexpression (GR-OX) or knockdown (GR-KD) on the tumor growth of iA2058- or iCOLO-679-bearing mice. Metastatic growth is shown in (A) and (B). Results obtained in these cells transfected with lentiviral vector not harboring any gene (GR-KD experiments) or empty plasmids (GR-OX experiments) (negative controls) were not different from control values. (C) Analysis of GR-OX and GR-KD were performed by measuring the GR content in melanoma cells. (D) GR-KD was also tested by western blot (a representative image is shown). Data are mean values ± SD from five to six different experiments (*$P < 0.05$, **$P < 0.01$, comparing RU486 treatment, GR-OX and GR-KD vs. controls).

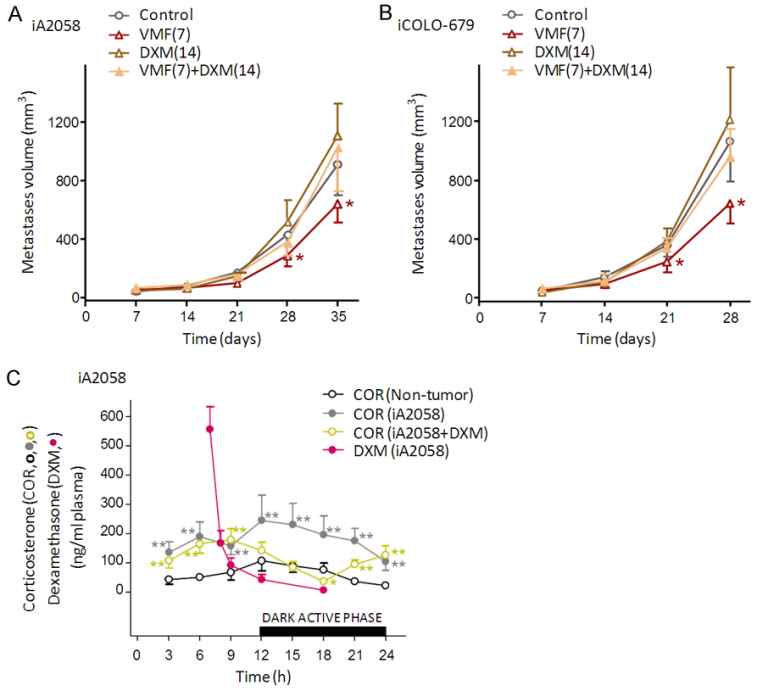

Figure 6. Effect of dexamethasone (DXM) and VMF administration on the tumor growth of (A) iA2058- or (B) iCOLO-679-bearing mice. VMF was administered for 3 weeks starting on day 7 after intradermic inoculation [VMF (7)] (as in **Figure 2**). DXM (0.2 mg/kg per day) was administered for 2 weeks starting on day 14 after inoculation. Data are mean values ± SD from 4-5 different experiments (*$P < 0.05$ comparing DXM and/or VMF treatment vs. controls). (C) Plasma levels of corticosterone (COR) in control non-tumor-bearing mice and in iA2058-bearing mice after DXM administration. Plasma levels of DXM were measured in iA2058-bearing mice after DXM administration. In these experiments DXM (0.2 mg/kg) was administered IV (one single dose) at 6 a.m. Blood was collected from the tail vein during the 24-h period. Measurement of corticosterone and DXM was performed as explained under Methods. Data are mean values ± SD from 6-7 different animals (*$P < 0.05$, **$P < 0.01$, comparing COR levels in tumor-bearing mice vs. controls).

ing melanoma patient-derived xenografts, tumor growth inhibition was observed when VMF was simultaneously administered with PD-0325901, a specific MEK inhibitor [27]. Nevertheless acquired resistance to MAPK pathway targeted therapies (BRAF/MEK inhibitors) develops in the majority of patients at approximately 12 months [28]. It has been also reported that the MEK/ERK signaling pathway regulates the expression of different Bcl-2-related proteins and promotes survival of e.g. human pancreatic cancer cells [29].

RU486 decreases the antioxidant defenses of melanoma cells and, thereby, increases ROS levels (**Table 1**). Higher ROS levels will favor metastatic cell damage and death (not protection against apoptosis). As shown above, histopathological studies revealed that RU486 administration causes

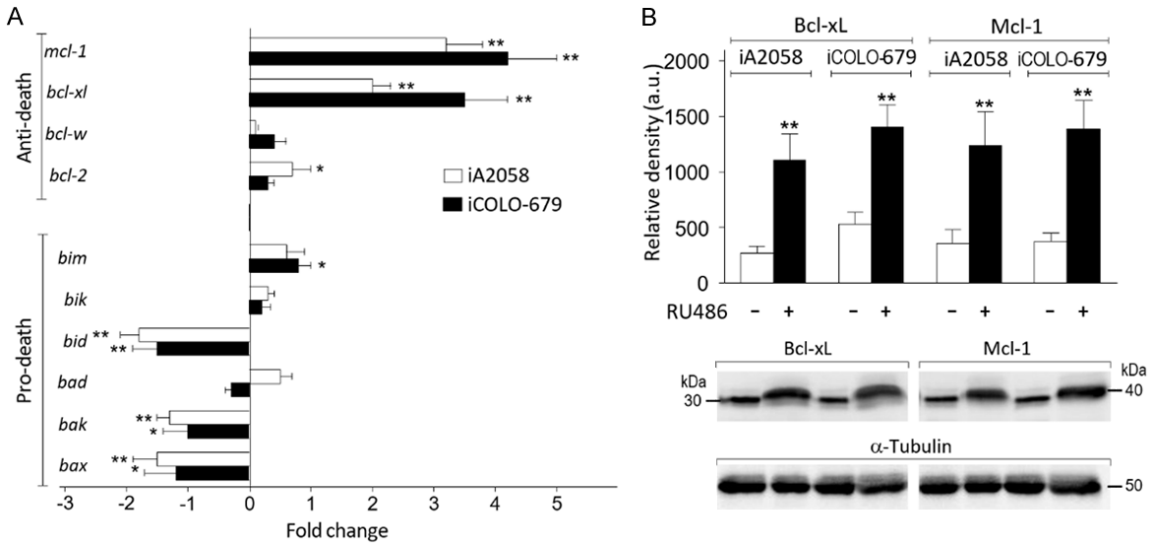

Figure 7. Effect of RU486 treatment on the expression (A) and levels (B) of Bcl-2 family proteins in metastatic BRAF^{V600E}-mutated melanoma cells isolated from *in vivo* growing tumors. iA2058 and iCOLO-679 cells were isolated 2 weeks after intradermic inoculation (see under Experimental procedures). The data, expressing fold change (quantitative RT-PCR) (A), show mean values ± SD for 5-6 different experiments (*P < 0.05, **P < 0.01 for all genes displayed comparing cells isolated from RU486-treated mice (as in **Figure 1**) vs. controls. Protein levels (western blots) (B) for selected anti-death Bcl-2-related proteins were measured in metastatic cells 14 days after inoculation (n = 4-5, **P < 0.01, comparing cells isolated from RU486-treated mice vs. controls).

a decrease in melanoma cell proliferation (Ki-67 staining) and an increase in apoptotic cell death (TUNEL) (**Figure 2**). However, paradoxically, surviving cells upregulate anti-death mechanisms (**Figure 3**). Therefore, it is possible that specific/pro-survival adaptations in the Bcl-2 family of proteins could be involved in the resistance showed by the growing metastatic melanoma cells (**Figure 3**). We found that mice bearing metastatic BRAF^{V600E}-mutated melanoma cells and treated with RU486, as compared to untreated controls, down regulate expression of different Bcl-2-related pro-death genes (i.e. *bax, bak, bid*); whereas upregulate anti-death *bcl-xl* and *mcl-1* (**Figure 7A**). Changes in gene expression equal or higher than 2-fold were further analyzed by western blotting (**Figure 7B**). Thus confirming that metastatic BRAF^{V600E}-mutated melanoma cells surviving the treatment with the antagonist of GR upregulate a specific Bcl-2-related anti-death defense.

Targeting of GR and Bcl-xL/Mcl-1 facilitates elimination of advanced BRAF^{V600E}-mutated melanoma metastases by vemurafenib

Our next step was to test if pharmacological inhibition of Bcl-xL or Mcl-1 could improve the results of the combined administration of RU486 and VMF in advanced melanoma. We used WEHI-539 (a recently developed Bcl-xL-selective BH3 mimetic) [30], and UMI-77 (a novel and selective small-molecule inhibitor of Mcl-1) [31]. RU486 was administered for 3 weeks starting one week after inoculation of the metastatic cells (early growing period), whereas VMF, WEHI-539 and/or UMI-77 were administered for two weeks starting two weeks after inoculation of the metastatic cells (advanced growing period).

Based on the results in **Figure 7**, it seems logic to think that Bcl-xl and Mcl-1 are main contributors of BRAF resistance. However, as shown in **Table 2**, the combined treatment of VMF and WEHI-539 and/or UMI-77 was not superior to VMF+RU486. Besides, the treatment with RU486+VMF+UMI-77 induced almost a complete regression of advanced BRAF^{V600E}-mutated iA2058 melanoma metastases (which overexpress *mcl-1* by approx. 3.2 fold and *bcl-xL* by approx. 2.0 fold as compared to mice treated only with RU486). In addition, the combined treatment with RU486+VMF+WEHI-77+UMI-77 was necessary to achieve metastases regression in mice bearing advanced BRAF^{V600E}-mutated iCOLO-679 melanoma metas-

Table 2. Effect of selective Bcl-xL or Mcl-1 inhibition on the efficacy of RU486 and vemurafenib against $BRAF^{V600E}$-mutated metastatic melanoma

	Metastases volume (mm^3)			
Treatment	iA2058		iCOLO-679	
Days after inoculation...	14	28	14	28
None	97 ± 36	421 ± 86	127 ± 35	955 ± 196
RU486	53 ± 17	147 ± 39**	84 ± 21	388 ± 117**
VMF (14)	85 ± 24	485 ± 116	116 ± 45	1061 ± 249
WEHI-539	74 ± 31	377 ± 112	133 ± 51	677 ± 155
UMI-77	66 ± 16	302 ± 94	149 ± 43	514 ± 147*
RU486 (14)+VMF (14)	57 ± 14	198 ± 57**	72 ± 18*	427 ± 101**
VMF (14)+WEHI-539	67 ± 25	355 ± 89	145 ± 61	615 ± 136
VMF (14)+UMI-77	55 ± 12	266 ± 75*	132 ± 74	474 ± 122*
WEHI-539+UMI-77	56 ± 26	240 ± 79**	102 ± 35	467 ± 106**
RU486+VMF (14)+WEHI-539	43 ± 15	155 ± 46**	96 ± 24	196 ± 63**
RU486+VMF (14)+UMI-77	51 ± 12	< 20**	65 ± 13**	155 ± 50**
VMF (14)+WEHI-539+UMI-77	51 ± 18	217 ± 83**	122 ± 50	403 ± 144**
RU486+VMF (14)+WEHI-539+UMI-77	62 ± 19	< 20**	77 ± 20*	< 20**

RU486 was administered as in **Figure 3**. VMF was administered as in **Figure 3** but starting 14 days after intradermic inoculation of the cancer cells. WEHI-539 (5 mg/kg IP, QD) (MCE, Monmouth Junction, NJ) and/or UMI-77 (50 mg/kg IV, QD) (Selleckchem, Houston, TX) wer e administered for 2 weeks also starting 14 days after inoculation of the cancer cells. WEHI-539 was dissolved in 10% DMSO, 40% PEG400, and 50% D5W. UMI-77 was dissolved in 10% DMSO, 70% Cremophor ELP, and 20% D5W. The volume administered to mice was, in both cases (WEHI-539 or UMI-77), < 50 mL. All data are mean values ± SD of 6-7 different animals in all groups (*$P < 0.05$; **$P < 0.01$ comparing all groups vs. controls).

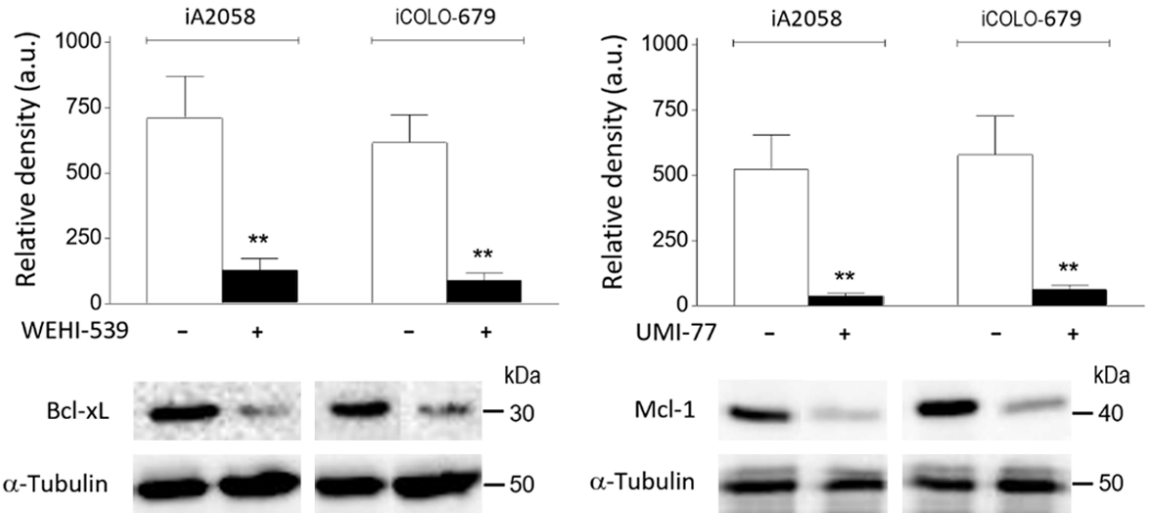

Figure 8. Downregulation of Bcl-xL and Mcl-1 by specific inhibitors. WEHI-539 and UMI-77 administration and western blots were performed as in **Table 2** (n = 4-5, **$P < 0.01$, comparing cells isolated from WEHI-539- or UMI-77-treated mice vs. controls).

tases (which overexpress *mcl-1* by approx. 4.2 fold and *bcl-xL* by approx. 3.5 fold as compared to mice treated only with RU486, **Figure 7A**; **Table 2**). WEHI-539-induced Bcl-xL downregulation and UMI-77-induced Mcl-1 downregulation were confirmed by western blot (see **Figure 8**). These results were validated using specific anti-*bcl-xl*-shRNA and anti-*mcl-1*-shRNA instead of the pharmacological inhibitors. As shown in **Table 3**, in mice bearing iA2058-*mcl-1*-shRNA melanoma cells treatment with RU486 and VMF causes a drastic decrease in metastases

Table 3. Effect of shRNA-induced selective Bcl-xL or Mcl-1 depletion on the efficacy of RU486 and vemurafenib against $BRAF^{V600E}$-mutated metastatic melanoma

Melanoma cell variants	Metastases volume (mm^3)	
Treatment	None	RU486+VMF (14)
iA2058	541 ± 151	257 ± 85#
iA2058-bcl-xl-shRNA	455 ± 120	179 ± 56#
iA2058-mcl-1-shRNA	449 ± 69	< 20*,#
iCOLO-679	833 ± 177	366 ± 91#
iCOLO-679-bcl-xl-shRNA	750 ± 155	156 ± 40*,#
iCOLO-679-mcl-1-shRNA	615 ± 103	130 ± 37*,#
iCOLO-679-bcl-xl-shRNA-mcl-1-shRNA	412 ± 112*	< 20*

RU486 was administered as in **Figure 3**. VMF was administered as in **Figure 3** but starting 14 days after intradermic inoculation of the cancer cells. Only melanoma cells treated with the specific shRNAs (see under Materials and Methods) were used in these experiments. Results obtained using melanoma cells treated with scrambled RNA sequences were not significantly different from those displayed as non-treated controls. All results displayed in the table correspond in all cases to metastases growth 28 days after intradermic inoculation. All data are mean values ± SD of 5-6 different animals in all groups (*$P < 0.05$ comparing iA2058 or iCOLO-679 control cells vs. their corresponding shRNA variants; #$P < 0.05$ comparing RU486+VMF-treated cells vs. non-treated cells).

Table 4. Effect of BRAF and MEK inhibitors on metastatic $BRAF^{V600E}$-mutated melanoma growth

	Metastases volume (mm^3)			
Treatment	iA2058		iCOLO-679	
Days after inoculation	14	28	14	28
None	126 ± 44	612 ± 184	135 ± 37	884 ± 206
RU486	78 ± 31	159 ± 41*	103 ± 36	317 ± 69*
VMF (14)	107 ± 32	577 ± 126	90 ± 29	954 ± 174
TRAM	145 ± 47	484 ± 134	147 ± 60	667 ± 196
COB	150 ± 52	749 ± 188	166 ± 55	1030 ± 284
RU486+VMF (14)	60 ± 27*	136 ± 37*	85 ± 21	384 ± 101*
VMF (14)+TRAM	50 ± 34*	317 ± 94*	73 ± 17*	414 ± 107*
VMF (14)+COB	93 ± 25	502 ± 106	116 ± 29	824 ± 169
RU486+VMF (14)+TRAM	53 ± 18*	99 ± 29*	61 ± 22*	148 ± 33*

VMF was administered as in **Figure 3** but starting 14 days after intradermic inoculation of the metastatic cells. Trametinib (TRA, GSK1120212) (0.3 mg/kg) and cobimetinib (COB) (5 mg/kg) were administered orally, daily (in a single dose) for 14 consecutive days, and also starting 14 days after intradermic inoculation of the metastatic cells. TRA (Selleckchem, Houston, TX) was reconstituted in 100 µL vehicle (methocel/polysorbate buffer). COB (Selleckchem) was dissolved in 75 µL of 0.5% hydroxypropyl methylcellulose and 0.2% Tween-80. All data are mean values ± SD of 5-6 different animals in all groups (*$P < 0.05$ comparing all groups vs. controls).

growth. A similar result was obtained in mice bearing iCOLO-679-*bcl-xl*-shRNA-*mcl-1*-shRNA melanoma cells treated with RU486 and VMF (**Table 3**). Thus suggesting that upregulation of specific anti-death Bcl-2-related proteins, such as Bcl-xL and/or Mcl-1 in the melanomas studied, may be key in the resistance of advanced $BRAF^{V600E}$-mutated metastases against RU486 and VMF.

Despite the efficacy shown by the combination of RU-486+VMF+specific anti-Bcl-2 therapy, at present, the BRAF-targeted therapy for melanoma is overwhelmingly dominated by the simultaneous use of BRAF+MEK inhibitors. Hence, we also tested in the efficacy of VMF and two different MEK1/2 inhibitors (cobimetinib, COB; and trametinib, TRAM) [32]. Both inhibitors were administered 14 days after inoculation of the metastatic cells (advanced growing period). Therefore, the conditions of advanced $BRAF^{V600E}$-mutated melanoma growth were as in **Table 3**. As shown in **Table 4**, metastatic growth was not significantly affected (as compared to controls) if any of the MEK inhibitors were administered alone. Combined administration of VMF and TRAM (not COB) significantly decreased melanoma growth (**Table 4**). Recently it was observed that VMF-resistant $BRAF^{V600E}$-mutated melanoma was also regressed by TRAM, but not COB, in a patient-derived orthotopic xenograft mouse model [33]. Combined administration of RU486+VMF+TRAM further decreased melanoma growth (**Table 4**), but was not as effective as the combination of RU486+VMF+specific anti-Bcl-2 therapy (**Table 2**).

As shown in **Figure 9**, survival was not significantly improved in metastatic melanoma-bearing mice treated with RU486, VMF or Bcl-xl and/or Mcl-1 inhibitors alone. Combination of RU486 and UMI-77 in iA2058-bearing mice or of VMF and WEHI-539+UMI-77 in iCOLO-679-bearing mice slightly improved survival

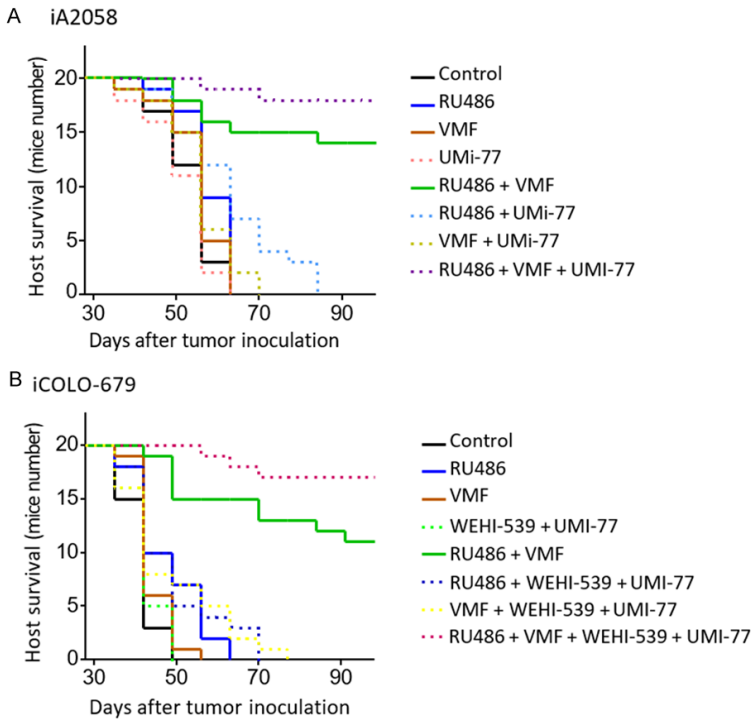

Figure 9. Effect of treatment-induced regression of metastatic melanoma growth on host survival. RU486 and VMF were administered, as in **Figure 3**, after intradermic inoculation of the cancer cells. WEHI-539 and UMI-77 were administered, as in **Table 1**, but from day 7 to day 28. Host survival was studied in the following treatment conditions: (-) physiological saline, (-) RU486, (-) VMF, (- -) UMI-77, (-) RU486+VMF, (- -) RU-486+UMI-77, (- -) VMF+UMI-77, (- -) RU486+VMF+UMI-77, (- -) WEHI-539+UMI-77, (- -) RU486+WEHI-539+UMI-77, (- -) VMF+WEHI-539+UMI-77, (- -) RU-486+VMF+WEHI-539+UMI-77. Data are means ± SD for 20 different mice in each experimental condition.

(**Figure 9**). However, treatment of melanoma-bearing mice (7 days after tumor inoculation, early growing period) with RU486+VMF significantly increased host survival (**Figure 9**). Whereas treatment of melanoma-bearing mice (14 days after inoculation, advanced growth) with RU486+VMF+Bcl-xl and/or Mcl-1 inhibitors further increased host survival (**Figure 9**).

Evaluation of drug-induced systemic toxicity

To evaluate potential side effects of the treatment regimens, standard hematology, clinical chemistry, and urinalysis were studied in non-tumor-bearing mice and in iA2058- and iCOLO-679-bearing mice, treated with vehicles or the combinations shown to induce melanoma growth inhibition. As shown in Table S2 (available on request from the corresponding author), tumor growth-related side effects included anemia, neutropenia, low NK cell count, and an increase of several tissue damage-related enzyme activities in plasma, including aspartate aminotransferase, alanine aminotransferase, GGT, alkaline phosphatase, and lactate dehydrogenase (all common in cancer patients).

Rates of glucose utilization by isolated hepatocytes and of glutamine and glucose by isolated $CD2^+$ lymphocytes were significantly increased in control melanoma-bearing mice as compared to non-tumor-bearing mice, although were found similar in control melanoma-bearing mice and in melanoma-bearing mice receiving full treatments (Table S2, available on request from the corresponding author). Thus suggesting that normal rates of utilization of main energy-supplying substrates are not compromised.

GSH levels in isolated hepatocytes or $CD2^+$ lymphocytes from control and treated melanoma-bearing mice were significantly decreased (Table S2, available on request from the corresponding author), although within levels expected in non-tumor-bearing mice subjected to 24 h fasting. This is a known tumor growth-derived effect associated to the interorgan GSH transport previously described in melanoma-bearing mice [34]. The cell volume of isolated hepatocytes or lymphocytes remained similar in cells isolated from non-tumor or tumor-bearing mice (Table S2, available on request from the corresponding author). All suggesting that these normal cells appear to preserve their physiological status. Moreover, when isolated hepatocytes from treated tumor-bearing mice and control non-tumor-bearing mice were cultured, their rates of growth were also similar.

These results clearly indicate that the toxicity caused by the treatments inducing metastatic melanoma growth inhibition, as compared to that associated to the tumor growth *per se*, appears clinically acceptable.

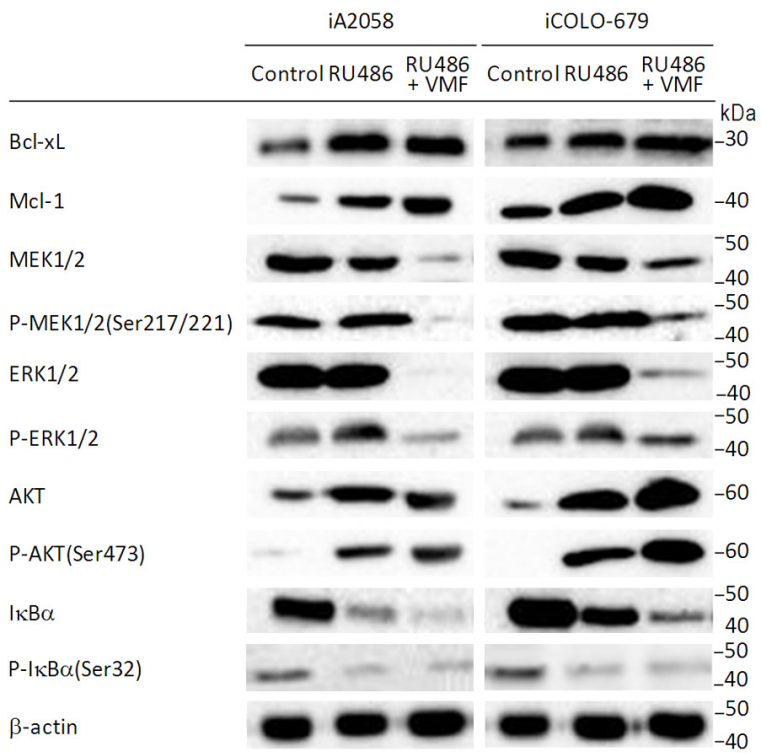

Figure 10. Effect of RU486 and VMF treatment on different Mcl-xL- and Mcl-1-related signaling pathways in growing metastatic melanoma cells. Melanoma-bearing mice were treated with RU486 and VMF as in **Figure 3**, but VMF was administered starting 2 weeks after tumor inoculation. Representative western blot of different signaling-related factors. *$P < 0.05$, **$P < 0.01$ comparing RU486- and/or VMF-treated mice vs. controls (mean values ± SD were calculated by densitometric analysis of n = 5-6 experiments, not shown).

Table 5. Effect of shRNA-induced selective AKT1 or NF-κB/p65 depletion on the efficacy of vemurafenib and RU486 against $BRAF^{V600E}$-mutated metastatic melanoma

Melanoma cell variants	Metastases volume (mm^3)		
Treatment	None	VMF	RU486+VMF
iA2058	502 ± 107	542 ± 125	254 ± 66$^{\#}$
iA2058-AKT1-shRNA	401 ± 88	236 ± 69$^{*,\#}$	84 ± 26$^{*,\#}$
iA2058-NF-κB/p65-shRNA	456 ± 112	279 ± 77$^{*,\#}$	33 ± 12$^{*,\#}$
iCOLO-679	867 ± 206	984 ± 236	375 ± 119$^{\#}$
iCOLO-679-AKT1-shRNA	755 ± 177	721 ± 159	55 ± 17$^{*,\#}$
iCOLO-679-NF-κB/p65-shRNA	708 ± 146	769 ± 186	91 ± 24$^{*,\#}$

VMF was administered as in **Figure 3** but starting 14 days after intradermic inoculation of the cancer cells. RU486 was administered as in **Figure 3**. Results obtained using melanoma cells treated with scrambled RNA sequences were not significantly different from those displayed as non-treated controls. All results displayed in the table correspond in all cases to metastases growth 28 days after intradermic inoculation. All data are mean values ± SD of 6-7 different animals in all groups ($^{*}P < 0.05$ comparing iA2058 or iCOLO-679 control cells vs. their corresponding shRNA variants; $^{\#}P < 0.05$ comparing VMF- or VMF+RU486-treated cells vs. non-treated cells).

Signaling pathways for modulation of Bcl-xL and Mcl-1 in advanced $BRAF^{V600E}$-mutated melanoma metastases

Upregulation of Bcl-xL and Mcl-1 expression in advanced $BRAF^{V600E}$-mutated melanoma metastases treated with RU-486 may overcome the BRAF/MEK/ERK signaling pathway. Thus resulting in resistance to VMF (**Figure 3**). In order to explore the underlying mechanism, we investigated potential alternatives, i.e. PI3K-PTEN-AKT- [26] and NF-κB-dependent signaling [35, 36]. As shown in **Figure 10**, treatment with RU486 results in an increase in Bcl-xL and Mcl-1 levels in metastatic $BRAF^{V600E}$-mutated melanoma cells isolated from *in vivo* growing tumors. This associates with a parallel increase in AKT, P-AKT and NF-κB binding to DNA, and a parallel decrease of IkBα and P-IkBα (**Figures 10** and S3, available on request from the corresponding author). Treatment with RU486 and VMF also causes a decrease in MEK1/2, P-MEK1/2, ERK1/2, and P-ERK1/2 without affecting the RU486-induced increase in AKT- and NF-κB-dependent signaling (**Figure 10**). Since the inhibitors of pan-PI3K signaling synergize with BRAF or MEK inhibitors to prevent BRAF-mutant melanoma cell growth [37], and the NF-κB pathway is activated in melanoma [22], our results suggest that PI3K-PTEN-AKT- and NF-κB-dependent signaling mechanisms may be responsible of the resistance-related adaptations involving Bcl-xL and Mcl-1 in advanced $BRAF^{V600E}$-mutated melanoma metastases. To validate this hypothesis we used

specific anti-AKT1-shRNA and anti-NF-κB/p65-shRNA. As shown in **Table 5**, melanoma resistance (associated to overexpression of Bcl-xL and Mcl-1) is decreased if AKT and NF-κB signaling pathways are blocked.

Discussion

GC, at the pathophysiological levels measured in plasma of tumor-bearing models, show tumor-promoting activities [7]. We have shown that GR knockdown decreases the expression of GCL and GSH, SOD1 and SOD2, CAT, GPX, and GSR in highly metastatic B16-F10 melanoma cells. Thus compromising their antioxidant protection and, thereby, causing a drastic decrease in their survival upon interaction with endothelial cells *in vitro* and *in vivo* [8]. Here we show that administration of a GR antagonist (RU486) to mice bearing metastatic $BRAF^{V600E}$-mutated melanoma cells also decreases the antioxidant protection (**Table 1**; **Figure 1**) and growth of melanoma cells (**Figure 1**). The RU-486-induced inhibition of melanoma growth could be reversed by experimentally inducing Nrf2 overexpression (**Figure 1**). Thus illustrating the importance of the Nrf2-mediated antioxidant defense system.

Production of large amounts of H_2O_2 by aggressive human tumor cells was first reported by Szatrowski and Nathan [38]. It is now well established that cancer promotion and progression is linked to oxidative stress, which causes DNA damage and mutations, genome instability, and abnormal cell proliferation [39]. Elevated ROS levels appear balanced by an increased antioxidant capacity (where Nrf2 plays a key role) within the cancer cells [40]. However an emerging concept postulates Nrf2 as a double-edged sword: Nrf2 is required for the protection of the body against cancer by endogenous and pharmacological anticancer agents; but at the same time, it is overactivated in different tumors, thus resulting in a prosurvival phenotype that favors tumor growth and resistance to oxidants and oncotherapy [41, 42]. DeNicola et al. [23] showed that Nrf2 deficiency impairs the development of KRAS- and BRAF-driven tumors. Moreover, it has been demonstrated that early-stage cancer cells lacking Nrf2 generate high ROS levels and exhibit a senescence-like growth arrest [23]. Moreover, besides oxidative stress-related genes, Nrf2 also controls expression of different heat-shock proteins, drug-efflux pumps and growth factors (all promoters of cancer resistance and/or growth) [43].

The tumor suppressor p53 (reduced, lost, or mutated in approx. half of all human cancers, particularly in highly aggressive and metastatic cancers) is activated by DNA damage and regulates the expression of many target genes leading to cell cycle arrest (thus allowing time for the repair of DNA damage) [44]. p53 can also interfere with the Nrf2-dependent transcription of ARE-containing promoters [45], and consequently loss of p53 associates with increased ROS levels [46]. We demonstrated, in metastatic B16 melanoma cells, that AS101 (an immunomodulator that increases expression of wild-type p53) caused a decrease in the expression of antioxidant enzymes [8]. Thus illustrating a cross-talk between p53 and Nrf2, and suggesting that p53 might be exploited by melanoma cells to gain protection against oxidative stress. Interestingly GR activation may inhibit p53-induced apoptosis, as it occurs in MCF-10Amyc cells via induction of protein kinase Cε [47]. Whereas in estrogen receptor-positive breast cancer low GR expression has been associated with higher p53 expression [48]. In fact wild-type p53 can physically interact with the GR forming a complex that results in cytoplasmic sequestration of both p53 and GR [49]. Therefore, a molecular link among GR, p53 and Nrf2 may be key in the underlying mechanism supporting growth and dissemination of $BRAF^{V600E}$-mutated melanoma cells.

VMF is used to treat adults with $BRAF^{V600E}$-mutated metastatic melanoma that cannot be surgically removed. It has been proven that VMF is effective at prolonging patients' lives and delaying the worsening of the disease. The main study showed that patients taking VMF lived on average for 13.2 months compared with 9.9 months for patients on dacarbazine, and it took on average 5.3 months for the disease to worsen in the VMF group compared with 1.6 months in the dacarbazine group (see e.g. [50]). Corazao-Rozas et al. reported that VMF increased mitochondrial respiration and ROS production in $BRAF^{V600E}$-mutated melanoma cell lines, and that melanoma cells showing acquired resistance to VMF displayed intrinsically high rates of mitochondrial respiration associated with elevated mitochondrial oxida-

tive stress [10]. Therefore, targeting of melanoma antioxidant defense could represent an effective strategy. As shown in **Figure 3**, combined administration of RU486 and VMF promotes regression of early melanoma metastases. However, a delay in VMF administration represented a loss of therapeutic efficacy (**Figure 3**). Thus suggesting additional adaptive mechanisms favoring melanoma cell survival, which were identified as Bcl-2 protein family-related mechanisms (Bcl-xL and Mcl-1 in the melanoma models used) [**Figures 7**, **10**; Table S2 (available on request from the corresponding author) and **Table 3**]. At present successful initial clinical trials of the BH3 mimetic venetoclax/ABT-199, specific for Bcl-2, have led to its recent licensing for refractory chronic lymphocytic leukemia and to multiple ongoing trials for other malignancies [51]. Moreover, preclinical studies herald the potential of emerging BH3 mimetics targeting other Bcl-2 pro-survival members, particularly Mcl-1, for multiple cancer types [51]. Thus suggesting that our findings may have clinical applications.

Acknowledgements

This research was supported by grants from the Ministerio de Economía y Competitividad (SAF2017-83458-R) (Spain), and from the University of Valencia (OTR2016-16618INVES) (Spain). C. L. Perez held a "Young Researchers" fellowship from the University of Valencia (Spain).

Disclosure of conflict of interest

None.

Address correspondence to: Elena Obrador, Department of Physiology, Faculty of Medicine and Odontology, University of Valencia, 15 Av. Blasco Ibañez, Valencia 46010, Spain. Tel: +34-963864-639; Fax: +34-963864642; E-mail: elena.obrador@uv.es

References

[1] Lo JA and Fisher DE. The melanoma revolution: from UV carcinogenesis to a new era in therapeutics. Science 2014; 346: 945-949.

[2] Jones C, Clapton G, Zhao Z, Barber B, Saltman D and Corrie P. Unmet clinical needs in the management of advanced melanoma: findings from a survey of oncologists. Eur J Cancer Care Engl 2015; 24: 867-872.

[3] Schlossmacher G, Stevens A and White A. Glucocorticoid receptor-mediated apoptosis: mechanisms of resistance in cancer cells. J Endocrinol 2011; 211: 17-25.

[4] Obradović MMS, Hamelin B, Manevski N, Couto JP, Sethi A, Coissieux MM, Münst S, Okamoto R, Kohler H, Schmidt A and Bentires-Alj M. Glucocorticoids promote breast cancer metastasis. Nature 2019; 567: 540-544.

[5] Zhang C, Wenger T, Mattern J, Ilea S, Frey C, Gutwein P, Altevogt P, Bodenmüller W, Gassler N, Schnabel PA, Dienemann H, Marmé A, Hohenfellner M, Haferkamp A, Pfitzenmaier J, Gröne HJ, Kolb A, Büchler P, Büchler M, Friess H, Rittgen W, Edler L, Debatin KM, Krammer PH, Rutz HP and Herr I. Clinical and mechanistic aspects of glucocorticoid-induced chemotherapy resistance in the majority of solid tumors. Cancer Biol Ther 2007; 6: 278-287.

[6] Herr I, Büchler MW and Mattern J. Glucocorticoid-mediated apoptosis resistance of solid tumors. Results Probl Cell Differ 2009; 49: 191-218.

[7] Volden PA and Conzen SD. The influence of glucocorticoid signaling on tumor progression. Brain Behav Immun 2013; 30 Suppl: S26-31.

[8] Obrador E, Valles SL, Benlloch M, Sirerol JA, Pellicer JA, Alcácer J, Coronado JA and Estrela JM. Glucocorticoid receptor knockdown decreases the antioxidant protection of B16 melanoma cells: an endocrine system-related mechanism that compromises metastatic cell resistance to vascular endothelium-induced tumor cytotoxicity. PLoS One 2014; 9: e96466.

[9] Mourah S, Denis MG, Narducci FE, Solassol J, Merlin JL, Sabourin JC, Scoazec JY, Ouafik L, Emile JF, Heller R, Souvignet C, Bergougnoux L and Merlio JP. Detection of BRAF V600 mutations in melanoma: evaluation of concordance between the Cobas® 4800 BRAF V600 mutation test and the methods used in French National Cancer Institute (INCa) platforms in a real-life setting. PLoS One 2015; 10: e0120232.

[10] Corazao-Rozas P, Guerreschi P, Jendoubi M, André F, Jonneaux A, Scalbert C, Garçon G, Malet-Martino M, Balayssac S, Rocchi S, Savina A, Formstecher P, Mortier L, Kluza J and Marchetti P. Mitochondrial oxidative stress is the Achille's heel of melanoma cells resistant to Braf-mutant inhibitor. Oncotarget 2013; 4: 1986-1998.

[11] Larkin J, Del Vecchio M, Ascierto PA, Krajsova I, Schachter J, Neyns B, Espinosa E, Garbe C, Sileni VC, Gogas H, Miller WH Jr, Mandalà M, Hospers GA, Arance A, Queirolo P, Hauschild A, Brown MP, Mitchell L, Veronese L and Blank CU. Vemurafenib in patients with BRAF (V600) mutated metastatic melanoma: an open-label,

multicentre, safety study. Lancet Oncol 2014; 15: 436-444.
[12] Benlloch M, Obrador E, Valles SL, Rodriguez ML, Sirerol JA, Alcácer J, Pellicer JA, Salvador R, Cerdá C, Sáez GT and Estrela JM. Pterostilbene decreases the antioxidant defenses of aggressive cancer cells in vivo: a physiological glucocorticoids- and nrf2-dependent mechanism. Antioxid Redox Signal 2016; 24: 974-990.
[13] Shimizu S, Eguchi Y, Kamiike W, Itoh Y, Hasegawa J, Yamabe K, Otsuki Y, Matsuda H and Tsujimoto Y. Induction of apoptosis as well as necrosis by hypoxia and predominant prevention of apoptosis by Bcl-2 and Bcl-XL. Cancer Res 1996; 56: 2161-2166.
[14] Buschmann D, González R, Kirchner B, Mazzone C, Pfaffl MW, Schelling G, Steinlein O and Reithmair M. Glucocorticoid receptor overexpression slightly shifts microRNA expression patterns in triple-negative breast cancer. Int J Oncol 2018; 52: 1765-1776.
[15] Qi Z, Whitt I, Mehta A, Jin J, Zhao M, Harris RC, Fogo AB and Breyer MD. Serial determination of glomerular filtration rate in conscious mice using FITC-inulin clearance. Am J Physiol Renal Physiol 2004; 286: F590-596.
[16] Berry MN and Friend DS. High-yield preparation of isolated rat liver parenchymal cells: a biochemical and fine structural study. J Cell Biol 1969; 43: 506-520.
[17] Thornton AM. Fractionation of T and B cells using magnetic beads. Curr Protoc Immunol 2003; Chapter 3: Unit 3.5A.
[18] Newsholme P, Gordon S and Newsholme EA. Rates of utilization and fates of glucose, glutamine, pyruvate, fatty acids and ketone bodies by mouse macrophages. Biochem J 1987; 242: 631-636.
[19] Dobos J, Kenessey I, Tímár J and Ladányi A. Glucocorticoid receptor expression and antiproliferative effect of dexamethasone on human melanoma cells. Pathol Oncol Res POR 2011; 17: 729-734.
[20] Sun Y, Fang M, Davies H and Hu Z. Mifepristone: a potential clinical agent based on its anti-progesterone and anti-glucocorticoid properties. Gynecol Endocrinol 2014; 30: 169-173.
[21] Homma S, Ishii Y, Morishima Y, Yamadori T, Matsuno Y, Haraguchi N, Kikuchi N, Satoh H, Sakamoto T, Hizawa N, Itoh K and Yamamoto M. Nrf2 enhances cell proliferation and resistance to anticancer drugs in human lung cancer. Clin Cancer Res 2009; 15: 3423-3432.
[22] Rocha CR, Kajitani GS, Quinet A, Fortunato RS and Menck CF. NRF2 and glutathione are key resistance mediators to temozolomide in glioma and melanoma cells. Oncotarget 2016; 7: 48081-48092.
[23] DeNicola GM, Karreth FA, Humpton TJ, Gopinathan A, Wei C, Frese K, Mangal D, Yu KH, Yeo CJ, Calhoun ES, Scrimieri F, Winter JM, Hruban RH, Iacobuzio-Donahue C, Kern SE, Blair IA and Tuveson DA. Oncogene-induced Nrf2 transcription promotes ROS detoxification and tumorigenesis. Nature 2011; 475: 106-109.
[24] Manzano JL, Layos L, Bugés C, de Los Llanos Gil M, Vila L, Martínez-Balibrea E and Martínez-Cardús A. Resistant mechanisms to BRAF inhibitors in melanoma. Ann Transl Med 2016; 4: 237.
[25] Sakakibara H, Koyanagi A, Suzuki T, Suzuki A, Ling L and Shimoi K. Effects of animal care procedures on plasma corticosterone levels in group-housed mice during the nocturnal active phase. Exp Anim 2010; 59: 637-642.
[26] Spagnolo F, Ghiorzo P and Queirolo P. Overcoming resistance to BRAF inhibition in BRAF-mutated metastatic melanoma. Oncotarget 2014; 5: 10206-10221.
[27] Monsma DJ, Cherba DM, Eugster EE, Dylewski DL, Davidson PT, Peterson CA, Borgman AS, Winn ME, Dykema KJ, Webb CP, MacKeigan JP, Duesbery NS, Nickoloff BJ and Monks NR. Melanoma patient derived xenografts acquire distinct Vemurafenib resistance mechanisms. Am J Cancer Res 2015; 5: 1507-1518.
[28] Welsh SJ, Rizos H, Scolyer RA and Long GV. Resistance to combination BRAF and MEK inhibition in metastatic melanoma: where to next? Eur J Cancer 2016; 62: 76-85.
[29] Boucher MJ, Morisset J, Vachon PH, Reed JC, Lainé J and Rivard N. MEK/ERK signaling pathway regulates the expression of Bcl-2, Bcl-X(L), and Mcl-1 and promotes survival of human pancreatic cancer cells. J Cell Biochem 2000; 79: 355-369.
[30] Lessene G, Czabotar PE, Sleebs BE, Zobel K, Lowes KN, Adams JM, Baell JB, Colman PM, Deshayes K, Fairbrother WJ, Flygare JA, Gibbons P, Kersten WJ, Kulasegaram S, Moss RM, Parisot JP, Smith BJ, Street IP, Yang H, Huang DC and Watson KG. Structure-guided design of a selective BCL-X(L) inhibitor. Nat Chem Biol 2013; 9: 390-397.
[31] Abulwerdi F, Liao C, Liu M, Azmi AS, Aboukameel A, Mady AS, Gulappa T, Cierpicki T, Owens S, Zhang T, Sun D, Stuckey JA, Mohammad RM and Nikolovska-Coleska Z. A novel small-molecule inhibitor of mcl-1 blocks pancreatic cancer growth in vitro and in vivo. Mol Cancer Ther 2014; 13: 565-575.
[32] Andrlová H, Zeiser R and Meiss F. Cobimetinib (GDC-0973, XL518). Recent Results Cancer Res 2018; 211: 177-186.
[33] Kawaguchi K, Murakami T, Chmielowski B, Igarashi K, Kiyuna T, Unno M, Nelson SD,

Russell TA, Dry SM, Li Y, Eilber FC and Hoffman RM. Vemurafenib-resistant BRAF-V600E-mutated melanoma is regressed by MEK-targeting drug trametinib, but not cobimetinib in a patient-derived orthotopic xenograft (PDOX) mouse model. Oncotarget 2016; 7: 71737-71743.

[34] Obrador E, Benlloch M, Pellicer JA, Asensi M and Estrela JM. Intertissue flow of glutathione (GSH) as a tumor growth-promoting mechanism: interleukin 6 induces GSH release from hepatocytes in metastatic B16 melanoma-bearing mice. J Biol Chem 2011; 286: 15716-15727.

[35] Grad JM, Zeng XR and Boise LH. Regulation of Bcl-xL: a little bit of this and a little bit of STAT. Curr Opin Oncol 2000; 12: 543-549.

[36] Liu H, Yang J, Yuan Y, Xia Z, Chen M, Xie L, Ma X, Wang J, Ouyang S, Wu Q, Yu F, Zhou X, Yang Y, Cao Y, Hu J and Yin B. Regulation of Mcl-1 by constitutive activation of NF-κB contributes to cell viability in human esophageal squamous cell carcinoma cells. BMC Cancer 2014; 14: 98.

[37] Sweetlove M, Wrightson E, Kolekar S, Rewcastle GW, Baguley BC, Shepherd PR and Jamieson SM. Inhibitors of pan-PI3K signaling synergize with BRAF or MEK inhibitors to prevent BRAF-mutant melanoma cell growth. Front Oncol 2015; 5: 135.

[38] Szatrowski TP and Nathan CF. Production of large amounts of hydrogen peroxide by human tumor cells. Cancer Res 1991; 51: 794-798.

[39] Panieri E and Santoro MM. ROS homeostasis and metabolism: a dangerous liason in cancer cells. Cell Death Dis 2016; 7: e2253.

[40] Gorrini C, Harris IS and Mak TW. Modulation of oxidative stress as an anticancer strategy. Nat Rev Drug Discov 2013; 12: 931-947.

[41] Hayes JD and McMahon M. The double-edged sword of Nrf2: subversion of redox homeostasis during the evolution of cancer. Mol Cell 2006; 21: 732-734.

[42] Jeddi F, Soozangar N, Sadeghi MR, Somi MH and Samadi N. Contradictory roles of Nrf2/Keap1 signaling pathway in cancer prevention/promotion and chemoresistance. DNA Repair 2017; 54: 13-21.

[43] Hayes JD and McMahon M. NRF2 and KEAP1 mutations: permanent activation of an adaptive response in cancer. Trends Biochem Sci 2009; 34: 176-188.

[44] Kansanen E, Kuosmanen SM, Leinonen H and Levonen AL. The Keap1-Nrf2 pathway: mechanisms of activation and dysregulation in cancer. Redox Biol 2013; 1: 45-49.

[45] Faraonio R, Vergara P, Di Marzo D, Pierantoni MG, Napolitano M, Russo T and Cimino F. p53 suppresses the Nrf2-dependent transcription of antioxidant response genes. J Biol Chem 2006; 281: 39776-39784.

[46] Sablina AA, Budanov AV, Ilyinskaya GV, Agapova LS, Kravchenko JE and Chumakov PM. The antioxidant function of the p53 tumor suppressor. Nat Med 2005; 11: 1306-1313.

[47] Aziz MH, Shen H and Maki CG. Glucocorticoid receptor activation inhibits p53-induced apoptosis of MCF10Amyc cells via induction of protein kinase Cε. J Biol Chem 2012; 287: 29825-29836.

[48] Abduljabbar R, Negm OH, Lai CF, Jerjees DA, Al-Kaabi M, Hamed MR, Tighe PJ, Buluwela L, Mukherjee A, Green AR, Ali S, Rakha EA and Ellis IO. Clinical and biological significance of glucocorticoid receptor (GR) expression in breast cancer. Breast Cancer Res Treat 2015; 150: 335-346.

[49] Yu C, Yap N, Chen D and Cheng S. Modulation of hormone-dependent transcriptional activity of the glucocorticoid receptor by the tumor suppressor p53. Cancer Lett 1997; 116: 191-196.

[50] Lee D, Porter J, Hertel N, Hatswell AJ and Briggs A. Modelling comparative efficacy of drugs with different survival profiles: ipilimumab, vemurafenib and dacarbazine in advanced melanoma. BioDrugs 2016; 30: 307-19.

[51] Cory S, Roberts AW, Colman PM and Adams JM. Targeting BCL-2-like proteins to kill cancer cells. Trends Cancer 2016; 2: 443-460.

Table S1. Genetic background of the melanoma cell lines used in this study

Gene	Melanoma cell lines		
	A2058	COLO-679	SK-Mel-28
BRAF	V600E	V600E	V600E
NRAS (exon 3)	WT	WT	WT
TP53	V274F	WT	145L/R
PTEN	+/-	+/-	+/-
CDKN2A	WT	WT	WT
CDK4	WT	WT	R24C

BRAF and CDK4 mutational status were determined by direct sequencing of PCR- amplified genomic fragments of exons 15 and 2, respectively. p53 mutational status was determined by direct sequencing of exons 2-10 by RT-PCR. PTEN levels were determined by immunoblotting and normalized to control melanocytes (+/- indicates no variation compared with human melanocytes). WT, wild type.

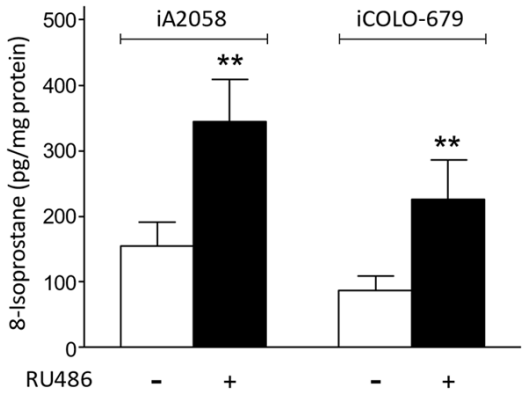

Figure S1. Effect of RU486 treatment on lipid peroxidation in metastatic human melanoma cells. 8-Isoprostane levels were measured to evaluate lipid peroxidation as indicated under Experimental procedures. Data are mean values ± SD of five to six different animals. $^{**}P < 0.01$, comparing RU486-treated mice vs. controls (as in **Table 1**).

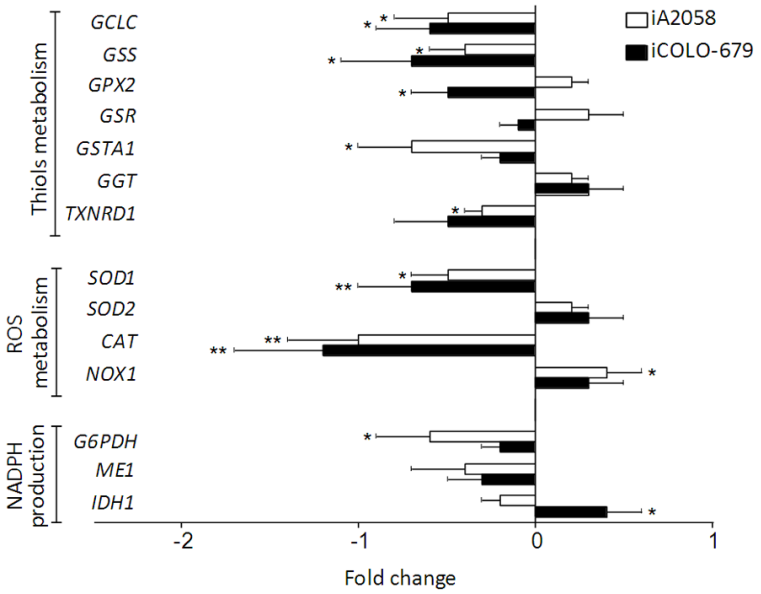

Figure S2. Effect of Nrf2 overexpression on the expression of different Nrf2-dependent genes in isolated iA2058 and iCOLO-679 cells from RU486-treated tumor-bearing mice. Tumor-bearing mice were treated with vehicle (controls) or RU486 as in **Table 1**. All data, expressing fold change (quantitative RT-PCR, see under Experimental procedures for calculations), show mean values ± SD for five to six different experiments. *$P < 0.05$, **$P < 0.01$ comparing RU486-treated tumor-bearing mice vs. control tumor-bearing mice treated with physiological saline.

Table S2. Hematology, clinical chemistry, and urinary balance data in metastatic human melanoma-bearing mice treated to induce metastases regression

	Non-tumor-bearing mice	Tumor bearing mice			
		iA2058		iCOLO-679	
		Control	RU486+VMF +UMi-77	Control	RU486+VMF++ WEHi-539+UMi-77
Hematology					
Hematocrit (%)	38.7 ± 1.8	33.5 ± 2.5	30.2 ±1.6**	30 ± 1.7**	27 ± 1.2**
Hemoglobin (g/dL)	12.3 ± 0.3	12.0 ± 0.5	11.2 ± 0.4*	11.2 ± 0.5*	10.2 ± 0.2**,#
Erythrocytes (10^6/mL)	8.5 ± 0.3	7.0 ± 0.1**	6.5 ± 0.2**,#	6.7 ± 0.2**	6.3 ± 0.1**
Platelets (10^3/mL)	412 ± 46	365 ± 70	260 ± 41**	333 ± 36*	170 ± 25**,##
Leukocytes (10^3/mL)	2.6 ± 0.3	2.5 ± 0.2	2.0 ± 0.2*#	2.4 ± 0.4	1.7 ± 0.1**,##
Lymphocytes (10^3/mL)	1.2 ± 0.3	1.3 ± 0.2	1.0 ± 0.1	1.2 ± 0.2	0.9 ± 0.15
% CD3	1.5 ± 0.1	1.2 ± 0.2	1.3 ± 0.1	1.1 ± 0.15*	1.1 ± 0.2*
% CD4	0.9 ± 0.1	1.0 ± 0.2	1.0 ± 0.2	0.7 ± 0.1*	0.8 ± 0.1
% CD8	0.3 ± 0.05	0.4 ± 0.1	0.3 ± 0.05	0.5 ± 0.2	0.3 ± 0.1
% B Cells	55.4 ± 7.8	47.7 ± 8.6	52.4 ± 5.4	42.4 ± 7.7	40.1 ± 6.3*
% NK	7.5 ± 1.2	3.8 ± 1.0**	4.2 ± 0.6**	4.1 ± 1.3**	5.0 ± 0.9**
Neutrophils (10^3/mL)	1.1 ± 0.2	0.5 ± 0.1**	0.5 ± 0.1**	0.4 ± 0.05**	0.5 ± 0.1**
Monocytes (10^3/mL)	0.1 ± 0.05	0.1 ± 0.05	0.1 ± 0.05	0.05 ± 0.02	0.15 ± 0.03
Eosinophils (10^3/mL)	0.05 ± 0.01	0.1 ± 0.02	0.05 ± 0.02	0.1 ± 0.05	0.05 ± 0.01
Basophils (10^3/mL)	0.0 ± 0.0	0.0 ± 0.0	0.0 ± 0.0	0.0 ± 0.0	0.0 ± 0.0
Plasma osmolarity (mOsm/kg)	296 ± 17	275 ± 11	312 ± 13##	345 ± 20	317 ± 14
Clinical chemistry					
Urea (mg/dL)	45.7 ± 5.1	55.6 ± 6.4	54.7 ± 5.7	59.3 ± 4.9**	56.4 ± 5.6*
Uric acid (mg/dL)	1.7 ± 0.2	1.9 ± 0.3	1.5 ± 0.3	2.2 ± 0.4*	1.7 ± 0.3
Total protein (g/dL)	4.2 ± 0.2	3.5 ± 0.1**	3.3 ± 0.4**	3.2 ± 0.5**	3.1 ± 0.2**

Albumin (g/dL)	3.0 ± 0.3	2.7 ± 0.4	2.5 ± 0.2	2.4 ± 0.5	2.5 ± 0.2
Creatinine (mg/dL)	0.4 ± 0.1	0.5 ± 0.1	0.6 ± 0.2	0.6 ± 0.1	0.5 ± 0.1
Glucose (mg/dL)	136 ± 15	174 ± 16*	155 ± 14	179 ± 20*	134 ± 17#
Total bilirubin (mg/dL)	0.5 ± 0.1	0.4 ± 0.05	0.4 ± 0.1	0.5 ± 0.2	0.4 ± 0.1
Direct bilirubin (mg/dL)	0.1 ± 0.01	0.05 ± 0.02	0.1 ± 0.01	0.1 ± 0.01	0.1 ± 0.01
Aspartate aminotransferase (IU/L)	125 ± 36	256 ± 21**	316 ± 46**	274 ± 29**	340 ± 38**
Alanine aminotransferase (IU/L)	7.7 ± 1.6	38.9 ± 9.7**	45.6 ± 17.4**	44.0 ± 12.9**	49.4 ± 15.6**
GGT (IU/L)	1.9 ± 0.3	4.2 ± 0.5**	4.1 ± 0.2**	3.7 ± 1.0**	4.6 ± 0.7**
Alkaline phosphatase (IU/L)	106 ± 21	144 ± 24	166 ± 17**	161 ± 29**	184 ± 30**
Lactate dehydrogenase (IU/L)	176 ± 37	425 ± 59**	517 ± 66**	460 ± 58**	477 ± 74**
Sodium (mEq/L)	155 ± 15	136 ± 24	115 ± 16	124 ± 23	130 ± 19
Potassium (mEq/L)	8.9 ± 1.3	9.2 ± 1.5	10.4 ± 1.1	10.7 ± 1.7	8.5 ± 2.0
Chloride (mEq/L)	91 ± 12	70 ± 14	62 ± 11*	78 ± 9	84 ± 16
Isolated hepatocytes					
GSH (nmol/g of cells)	6243 ± 326	3504 ± 244**	3009 ± 491**	3017 ± 204**	2508 ± 317**
Cell volume (mL/mg dry wt.)	3.1 ± 0.3	3.2 ± 0.2	3.0 ± 0.4	3.0 ± 0.1	2.9 ± 0.3
Glucose utilization (mmol/g x min)	1.55 ± 0.33	2.14 ± 0.15**	1.66 ± 0.21##	2.49 ± 0.22**	1.59 ± 0.16##
Isolated *CD2+lymphocytes*					
GSH (nmol/10^6 cells)	5.6 ± 1.1	2.7 ± 0.6**	2.2 ± 0.9**	2.5 ± 0.5**	2.0 ± 0.4**
Cell volume (mm^3)	161 ± 24	145 ± 17	147 ± 21	155 ± 26	150 ± 18
Glucose utilization (mmol/g x min)	1.76 ± 0.20	2.40 ± 0.15**	1.84 ± 0.17##	2.80 ± 0.23**	2.04 ± 0.22##
Glutamine util. (mmol/g x min)	3.40 ± 0.17	4.50 ± 0.49**	4.05 ± 0.42*	4.06 ± 0.33**	3.81 ± 0.55
Urinary balance					
pH	7.5 ± 0.3	7.8 ± 0.4	8.2 ± 0.3*	7.7 ± 0.5	7.8 ± 0.2
Leukocytes (mL^{-1})	Negative	Negative	Negative	Negative	Negative
Erythrocytes (mL^{-1})	Negative	Negative	Negative	Negative	Negative
Nitrite	Negative	Negative	Negative	Negative	Negative
Protein (g/L)	0.2	0.2	0.4	0.2	0.2
Glucose	Normal	Normal	Normal	Normal	Normal
Ketones	Negative	Negative	Negative	Negative	Negative
Urobilinogen	Normal	Normal	Normal	Normal	Normal
Bilirubin	Negative	Negative	Negative	Negative	Negative
GFR (mL/min)	188 ± 36	171 ± 25	177 ± 27	164 ± 33	169 ± 18

Full treatment means the combination of RU486+VMF+UMI-77 in iA2058-bearing mice and of RU486+VMF+WEHI-539+UMI-77 in iCOLO-679-bearing mice. Standard cell count and chemistry were measured in peripheral blood samples taken from the saphena vein. Data are means ± SD for 7-8 different mice in each experimental condition. *P < 0.05 and **P < 0.01 comparing tumor-bearing mice vs. non-tumor-bearing mice. #P < 0.05 and ##P < 0.01 comparing, under tumor-bearing mice, full treatment vs. treatment with vehicles.

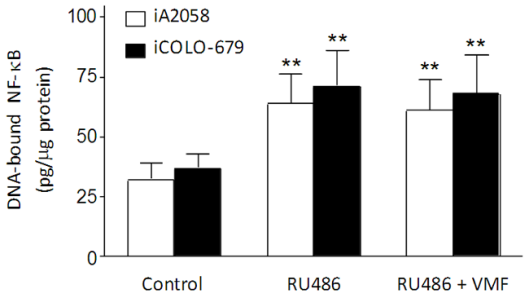

Figure S3. Effect of RU486 and VMF treatment on different Mcl-xL- and Mcl-1-related signaling pathways in growing metastatic melanoma cells. Melanoma-bearing mice were treated with RU486 and VMF as in **Figure 3**, but VMF was administered starting 2 weeks after tumor inoculation. NF-κB binding to DNA (data are mean values ± SD of 4-5 different animals in all groups; **P < 0.01 comparing RU486- and/or VMF-treated mice vs. controls).